SOIL ORGANISMS 88 (2) · August 2016 pp. 111–132

Fine structural observations of the erectile setae and dermal glands on the notogaster of *Heterochthonius gibbus* (Oribatida, Enarthronota, Heterochthoniidae)

Gerd Alberti[1,*] and Ana Isabel Moreno Twose[2]

[1] Zoologisches Institut und Museum, E-MAU Greifswald, J.-S.-Bach-Str. 11/12, 17489 Greifswald, Germany
[2] Communidad de Baleares 8, 31010 Barañain, Spain
* Corresponding author, e-mail: alberti@uni-greifswald.de

Received 28 December 2015 | Accepted 22 April 2016
Published online at www.soil-organisms.de 1 August 2016 | Printed version 15 August 2016

Abstract

The external and internal structures of the notogaster of the enarthronote oribatid mite *Heterochthonius gibbus* are described, focused on the apodemal and muscular structures involved in the erection of setae. A functional model is suggested to explain the peculiar defensive movements of the setae. This model concerns the structure and deformation of the intercalary sclerites due to contraction of peculiar non-striated muscles that stretch between apodemal ribs bordering the relevant sclerites. Innervation of each of the setae on the anterior notogaster occurs by two dendrites of mechanosensitive cells. Four pairs of dermal glands are described for the first time from an enarthronote oribatid mite. These glands deliver a complex secretion on the external surface of the mite. A detailed scheme of the arrangement of setae, sclerites and scissures of the notogaster of *H. gibbus* is presented.

Keywords Enarthronotides | glands | movable setae | non-striated muscle cells | scissures | sclerites | ultrastructure

1. Introduction

Heterochthonius gibbus is a rarely observed oribatid mite belonging to Heterochthoniidae, a family of isolated taxonomic position within the group of Enarthronota (= Enarthronotides; Grandjean 1954, Norton & Behan-Pelletier 2009). Besides its three prodorsal eyes, a feature occurring rarely in Oribatida (Grandjean 1928, Alberti & Moreno-Twose 2012), it is well-known because of its erectile dorsal setae situated on the dorsal hysterosoma or notogaster (Grandjean 1928, 1931, 1947, 1948, Norton 2001, Weigmann 2001, 2006, Norton & Behan-Pelletier 2009). Grandjean (1931) suggested that, like in *Cosmochthonius* sp., the setae of *H. gibbus* are indirectly erected by peculiar tilting movements of the intercalary sclerites on which these setae are positioned on the dorsal hysterosoma (Fig. 1). These tilting movements should be caused by a dilatation or contraction of the hysterosoma. The forces inducing these movements were not mentioned. However, he stated that there are no muscles inserting directly on the setae. In 1994, Alberti and Moreno (personal communication) observed muscles between the dorsal sclerites that likely should be involved in these setal actions (Alberti & Coons 1999, see also Norton 2001). Here we describe these muscles and sclerites in more detail including some remarks on other notogastral structures and reporting the presence of rather large dermal glands not observed before in Enarthronota.

2. Materials and methods

About 20 specimens of *Heterochthonius gibbus* (Berlese, 1910) were collected near Grindelwald (Switzerland) in summer 1994 from a rotten tree-stump at about 1500 m

ISSN 1864-6417

above s.l. from samples extracted with Berlese-funnels. They were further processed as follows:

Living specimens were kept in small boxes with a bottom of Plaster of Paris. They were observed under an Olympus stereomicroscope connected with a Sony video-camera at the University of Vechta (Germany).

Subsequently, a number of specimens were transferred to 70 % ethanol. These specimens were used for scanning electron microscopy (SEM). Some were broken into pieces to reveal internal peculiarities. The specimens were dehydrated using graded ethanols, transferred into dichlordifluormethan, critical point dried using liquid CO_2 as final medium. They were mounted on Al-stubs, coated with gold and examined with a Philips SEM 505 and a LEO DSM 940A.

For transmission electron microscopy (TEM), specimens were transversely cut into halves and fixed in ice-cold 3.5 % glutaraldehyde (pH 7.4, phosphate buffer 0.1M) for two hours. After rinsing with buffer solution, the tissues were postfixed with 2 % OsO_4 aqueous solution. After rinsing again, specimens were dehydrated with graded ethanols and embedded in Araldite using propylenoxide as intermedium. Ultrathin sectioning (70 nm) was done with a Leica UCT using a Diatome diamond knife. Sections were done in transversal, horizontal (frontal) and sagittal plane using five specimens, which turned out to be all males. 100 mesh copper grids provided with a Pioloform-film were used to bear the sections. The sections were stained with uranylacetate and lead citrate (Reynolds 1963) and studied with a JEOL JEM-1011 transmission electron microscope. For general orientation semithin sections (400 nm) were stained according to Richardson et al. (1960) and studied with a compound light microscope (LM). For more technical information see Alberti & Nuzzaci (1996a).

3. Results and Discussion

3.1. Observation of living mites

Living *Heterochthonius gibbus* mites are quite fast running in the rearing chamber. They are amber-like coloured with large lustrous and glassy notogastral setae lying parallel to the surface of the body. When touched with a needle, some of the notogastral setae were suddenly and apparently simultaneously erected and also spread sidewards. This erection was evident in the two posterior rows of macrosetae. When disturbance was stopped, the setae slowly moved down returning to their original position (see video supplement on www.soil-organisms.org; Figs 1, 2A, B).

3.2. External aspects

In *Heterochthonius gibbus* the dorsal region of the hysterosoma, i.e. the notogaster – as a general feature in Enarthronota – is divided into several transversal sclerites that are separated by scissures (Figs 1, 2). In *H. gibbus* three transversal scissures in the anterior half of the hysterosoma separating three transversal, rather broad sclerites are reported (Grandjean 1928, Norton 2001). The third, posterior scissure separates the third sclerite from the undivided posterior notogaster (or fourth sclerite; numbers of sclerites according to Grandjean 1931). Each of the sclerites 1-3 slightly overlaps the following one. The notogaster bears transversal rows of setae, which are denoted as rows *c, d, e, f, h* and *p*. All these setae are positioned into flexible sockets (Fig. 2). The first 4 rows are located in the anterior half of the notogaster, the rows *h* and *p* are at the posterior end of the notogaster. These posterior setae are not considered further here.

Grandjean (1947) distinguished between several types of scissures separating sclerites. In *H. gibbus* the first scissure (between the first and the second sclerite) is described as a simple articulation, termed type E scissure (Grandjean 1947, Norton 2001, Norton & Behan-Pelletier 2009) and composed of a band of thin flexible cuticle between the thicker sclerotized sclerites. However, as stated above, the first sclerite slightly overlaps the second with its posterior border (see also below). Hence a tendency towards formation of a small posterior tectum (an external, protective prolongation of the exoskeleton; Grandjean 1934, Hammen 1980) is certainly present. A scissure with a pronounced tectum was designated as a type L scissure by Grandjean (1947, see also Norton 2001). The two posterior scissures are provided with four small so-called intercalary sclerites each bearing a macroseta. Such scissures represent the third type of scissures, the type S scissure (Grandjean 1947, see also Norton 2001, Weigmann 2001, 2006).

However, these intercalary sclerites – typical for the type S scissures – seem according to our observations not to be real separate platelets. Instead our SEM-figures only show posterior indentations between the setae-bearing areas and a very narrow and fine line (thin furrow and/or rib) in front of the rows of setae e and f. This line is much less distinct than that forming scissure 1 in front of setal row d or the deep transversal indentations posterior of setae e and f (compare Figs 2D–H). We thus think that these indentations – posterior of setae e and f – are the 'real' scissures separating sclerites 2 and 3 and 3 and 4. Consequently, we interpret the so-called intercalary sclerites as being evolved as a specialization from posterior tectum-like borders of type L scissures as it is still (weakly) present in the first scissure of *H. gibbus.*

The notogaster bears paired setae in transversal rows, which are counted laterad starting from the median axis (Figs 1, 2). At maximum one row comprises three setae on each side of the hysterosoma (Weigmann 2001, 2006). The first sclerite, located immediately behind the dorsosejugal furrow, bears a row of four medium-size setae anteriorly. These setae, denoted as row *c*, are rather thin, finely and densely pilose. They are positioned on two transversal bars of elevated cuticle that are medially separated by a distinct gap. In addition to these four (*c2, c1, c1, c2*) slender and pilose setae (100 µm), there is a very tiny smooth seta (13 µm) more lateroventrally on each side, which is also

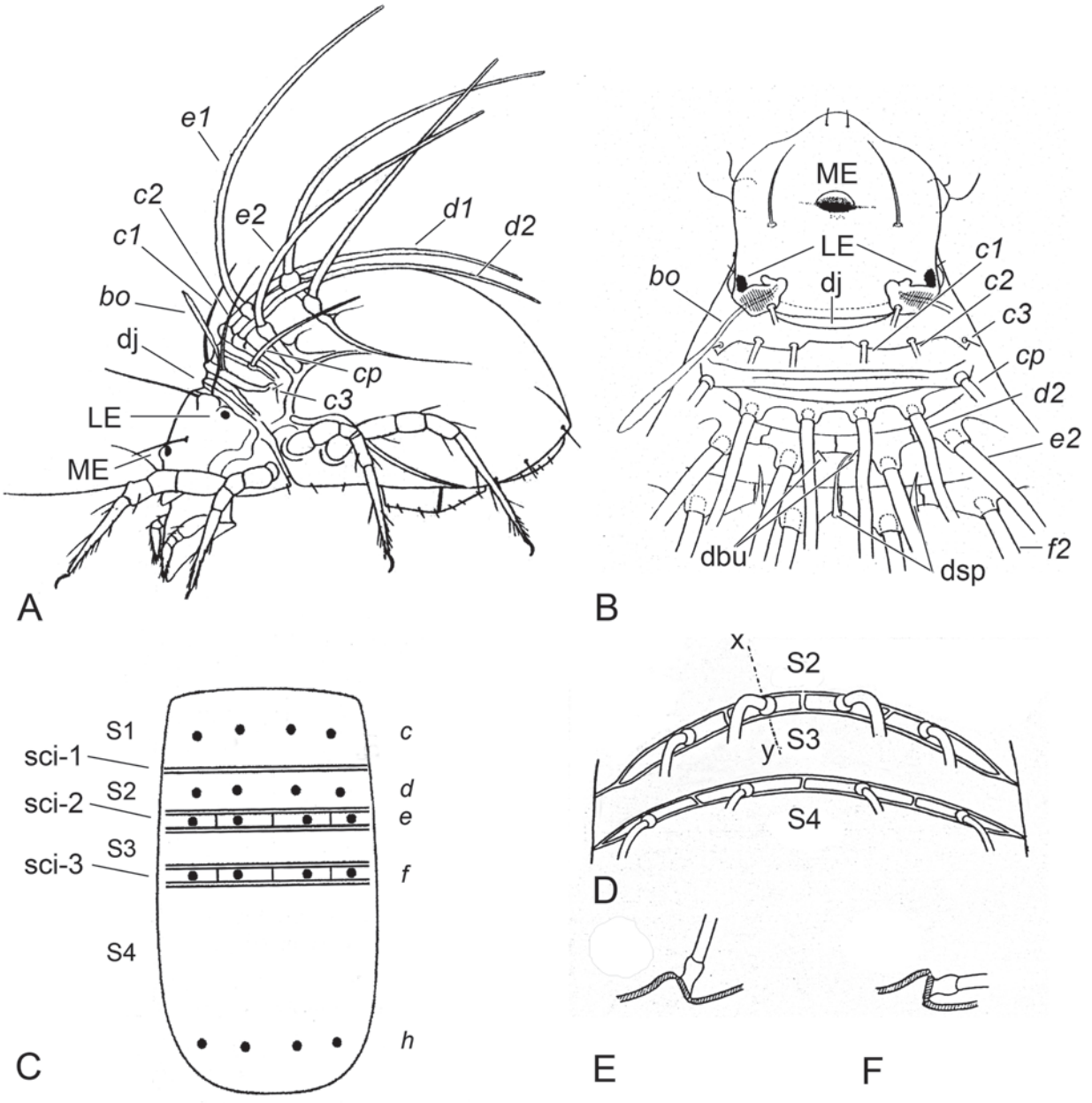

▲ **Figure 1**. Drawings showing external features of *Heterochthonius gibbus* (A, B, D–F modified from Grandjean 1928, 1931; C modified from Norton 2001). (**A**) Lateral view of *H. gibbus* showing setae of left side of body. (**B**) Dorsal view of anterior part of body. (**C**) Scheme of sclerites, and scissures with setation on dorsal hysterosoma (notogaster) (only most dorsal setae shown; i.e. setae *c3*, *cp* and *p* are omitted). (**D–F**) Erectile setae of *Cosmochthonius* sp. and mechanism of their movement as suggested by Grandjean (1931). The line joining x-y is line of section through intercalary sclerite shown in E (erected seta) and F (laid down seta).

Abbr.: ***bo*** – bothridial seta (trichobothrium), ***c***, ***c1***, ***c2***, ***c3*** – setae of row *c*, ***cp*** – setae *cp*, ***d1***, ***d2*** – setae of row *d*, **dj** – dorsosejugal furrow, **dbu** – dorsal bumps, **dsp** – dorsal spines, ***e1***, ***e2*** – erectile setae of row *e*, ***f1***, ***f2*** – erectile setae of row *f*, **LE** – lateral eye, **ME** – median eye, **S1-4** – dorsal sclerites 1-4, **sci-1** – anterior scissure (= type E scissure), **sci-2** – median scissure (= type S scissure with intercalary sclerites), **sci-3** – posterior scissure (= type S scissure with intercalary sclerites).

counted as a member of row *c* (*c3*) (Figs 1A, B, 2C). It is placed on a slight posteriorly directed elevation of the mentioned cuticular bars. Posterior of this row *c*, a distinct transversal depression is evident dividing the first sclerite into an anterior part bearing setal row *c* and a posterior region that bears only one pair of setae at its lateral ends (Figs 1A, B, 2A–D). These setae are much larger (125 µm) than the *c3* setae but much smaller than the macrosetae of rows *d, e, f*. These lateral setae termed *cp* by Grandjean (1947) are considered to belong to the following row *d* of setae (and hence denoted *d3*) by Weigmann (2001, 2006). However, as is evident from Fig. 2C, these setae (*cp/d3*) are positioned distinctly in front of the following scissure that separates sclerite 2 bearing setae *d1, d2* from sclerite 1 bearing *c1, c2*. We hence consider this pair of setae as being separated from the setal row *d* and hence prefer the denotation *cp*. This pair of setae is also positioned on slight elevations of the cuticle.

The three dorsal rows (*d, e, f*) following posteriorly row *c* (and pair *cp*) are composed of four setae. Each of these setae shows an appearance rather similar to the two lateral setae (*cp*), but being conspicuously thicker and longer (Figs 1A, B, 2A–F). These macrosetae reach the posterior end of the mite (all setae *d, e, f* about 300 µm long) and are also placed on distinct elevations. They appear rather smooth with a sparse pilosity. The setae *d1, d2* show basally a slight undulating shape as already mentioned by Grandjean (1928) (Figs 1B, 2E). As a peculiarity, the macrosetae of the two posterior rows *e* and *f* are usually described as not being placed on broad sclerites. Instead, these setae are positioned on the so-called intercalary sclerites of the type S scissures as discussed above (Grandjean 1928, 1947, Norton 2001, Weigmann 2001, 2006) (Figs 1A–C, 2D–F). In *H. gibbus* these setae (row *e* and *f*) are distinctly movable or erectile.

According to the studies of Grandjean (1928, 1947, see also Norton 2001, Weigmann 2001, 2006), a sclerite (i.e. sclerite 3) bearing no setae is located between rows *e* and *f*. However, according to our interpretation setal row *f* belongs to this sclerite.

It is broadly accepted that these rows of setae indicate a fundamental segmental organization of the hysterosoma of actinotrichid (acariform) mites (e.g., Grandjean 1939, Hammen 1963, 1970, 1989, Evans 1992). The segments are denoted with the according capital letters C, D, E, F, H, P (or PS), AD, AN. Here we discuss only the region of segments C–H.

When a *H. gibbus* mite is in rest, all these setae are kept close to the body, being slightly bent parallel to the body surface. As mentioned above, the mite on disturbance quickly arises and spreads the macrosetae of the posterior rows *e* and *f* evidently as a defensive reaction. We think that the small posterior indentations between the so-called intercalary sclerites in one row are flexible regions that allow the sideward spreading of the macrosetae *e* and *f*. Some SEM-figures (Fig. 2A, B) suggest that setae *d1, d2* may also be slightly erected, but not as significantly as rows *e* and *f*. Since these setae of row *d* are placed on a common cuticular rib (Fig. 2F) and not on intercalary sclerites, they likely cannot be spread sidewards.

Three notogastral spines project anteriorly from the undivided notogaster (sclerite 4) passing across the scissure between the posterior sclerite and the undivided rest of the notogaster. The median spine is the largest (Grandjean 1928, Weigmann 2006). In front of the median spine two small, slightly pointed bumps project from sclerite 3 towards scissure 2 (Figs 2D, E, 3A, B).

We observed for the first time 3 pairs of tiny pores on the notogaster (Figs 2D, F–H). One pore is located lateral of the base of seta d1 (Fig. 2F, H), another one was found on sclerite 3 in front of seta f2 (Fig. 2 D, G), and a third pore was seen on sclerite 4 just behind scissure 3 and approximately between the lateral spine and seta f2 (Fig. 2D, G). The surface of the body of some of the studied specimens is at least partly covered by a secretion (Fig. 2D, E).

3.3. Internal aspects

Setae: The setae are largely massive structures being only 'hollow' at their bases close to their insertions (Figs 4, 5, 8D, E). From here a thin strand of denser material runs through each seta and likely represents the line of retraction of the trichogen cell (Figs 4D, 5B, G, 8D, E, F). In cross sections the setae consist mainly of a rather electron-lucent cuticle, only a thin layer of dense material was seen in the periphery. The electron-lucent cuticle resembles that observed in the oribatid mite *Archegozetes longisetosus* as likely representing the birefringent material (Alberti et al. 2011). However, it is evident from the broken setae seen in some SEM-preparations that the setae are centrally less dense and solid than in their periphery (Fig. 3A), what may correspond to the different appearance of these regions in the polarized light as reported from the recently described enarthronote species *Nanohystrix hammerae* (Norton & Fuangarworn 2015). All setal bases we could observe are movably inserted into sockets with the setal base surrounded by suspension fibers, into which a pair of dendrites terminates with large tubular bodies (Figs 2C–H, 3A, B, 4, 5, 8A, D, E, F). The microtubules of the tubular bodies are interconnected and are in contact with the dendritic membrane by tiny dense bars that resemble the small cones known from insect mechanorecptors as being probably important for stimulus transduction

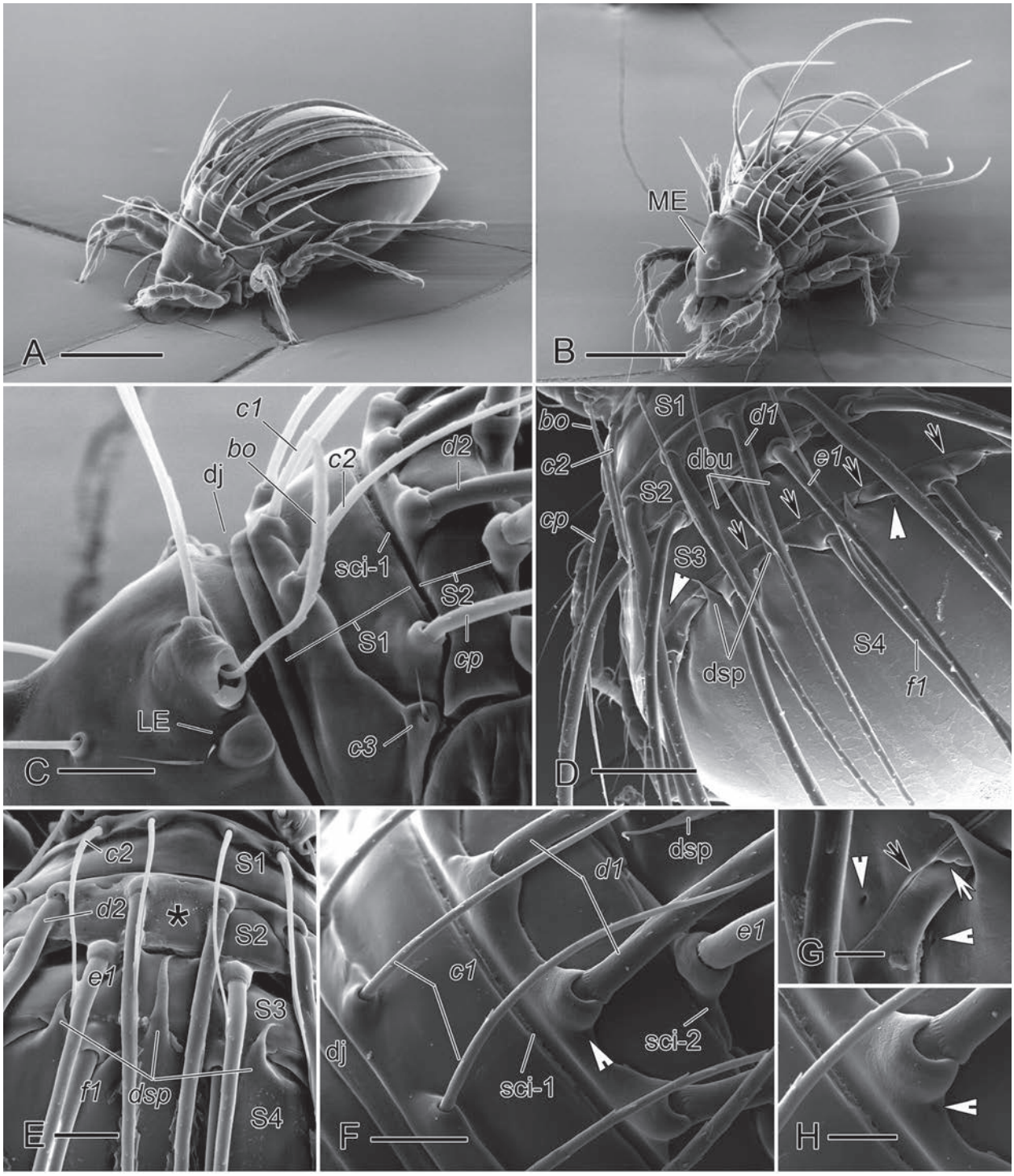

▲ **Figure 2**. SEM-figures of *Heterochthonius gibbus*. (**A, B**) Setae in rest and erected. Note that posterior setae (rows *e* and *f*) are most erected and also spread sidewards in B. Scale bars: 100 µm. (**C**) Lateral view of body region close to dorsosejugal furrow, showing anterior notogastral sclerites and setae. Note tiny seta *c3*. Scale bar: 25 µm. (**D**) Dorsoposterior view on notogaster. White arrowheads point to orifices of dermal glands, black arrows indicate thin line of flexibility (= anterior border of intercalary sclerites or type S-scissure) in front of erectile setae *f*. Scale bar: 50 µm. (**E**) Posterior view on notogaster showing dorsal spines. Note that sclerite 2 is partly covered by secretion (asterisk). Setae *d2* show undulating shape basally. Scale bar: 25 µm. (**F**) Dorsolateral view on notogaster with pore of dermal gland (white arrowhead) behind scissure 1 (= type E scissure). Scale bar: 50 µm. (**G**) Part of scissure 3 (= type S scissure). White arrowheads point to orifices of dermal glands. Black arrow indicates thin line of flexibility line, white arrow points to posterior incision between two intercalary sclerites. Scale bar: 10 µm. (**H**) Detail of F showing dermal gland orifice (white arrowhead) in higher magnification. Scale bar: 10 µm.

Abbr.: ***bo*** – bothridial seta (trichobothrium), ***c1***, ***c2***, ***c3*** – setae of row *c*, ***cp*** – seta *cp*, ***d1***, ***d2*** – setae of row *d*, **dbu** – dorsal bumps, **dj** – dorsosejugal furrow, **dsp** – dorsal spines, ***e1*** – erectile seta of row *e*, ***f1*** – erectile seta of row *f*, **LE** – lateral eye, **ME** – median eye, **S1-S4** – dorsal sclerites S1-S4, **sci-1** – scissure 1 (= type E scissure), **sci-2** – scissure 2 (= type S scissure).

(Fig. 5G; Keil & Steinbrecht 1984, Thurm 1984). Thus these setae present mechanoreceptive structures. The cuticle of the socket provided with half-round densities extends as a dendritic sheath into the interior of the mite for some distance and finally disintegrates into irregular dense sheets surrounded by the thecogen cell (Fig. 5I–L). The sensory cells are composed of outer and inner dendritic segments that are separated by a short ciliary segment containing basal bodies as typical for such sensilla (Fig. 5; Keil & Steinbrecht 1984, Thurm 1984). The more proximal regions of the sensory cells were not studied.

The surface of the setae is finely striated and is covered by a thin layer of external material (Figs 2H, 4A, D, 5B, C).

Large cells, which possess apically long and densely packed microvilli, appeared rather peculiar to us (Fig. 6). The cells contain many lipid inclusions, some lysosomes, a rather large heterochromatin-poor nucleus and long mitochondria. These cells are found close to the dendrites innervating the setae. The ducts of the dermal glands (see below) also pass often through these tissues. However, these conspicuous cells likely represent auxiliary cells of the setal complex, i.e. tormogen and trichogen cells, and

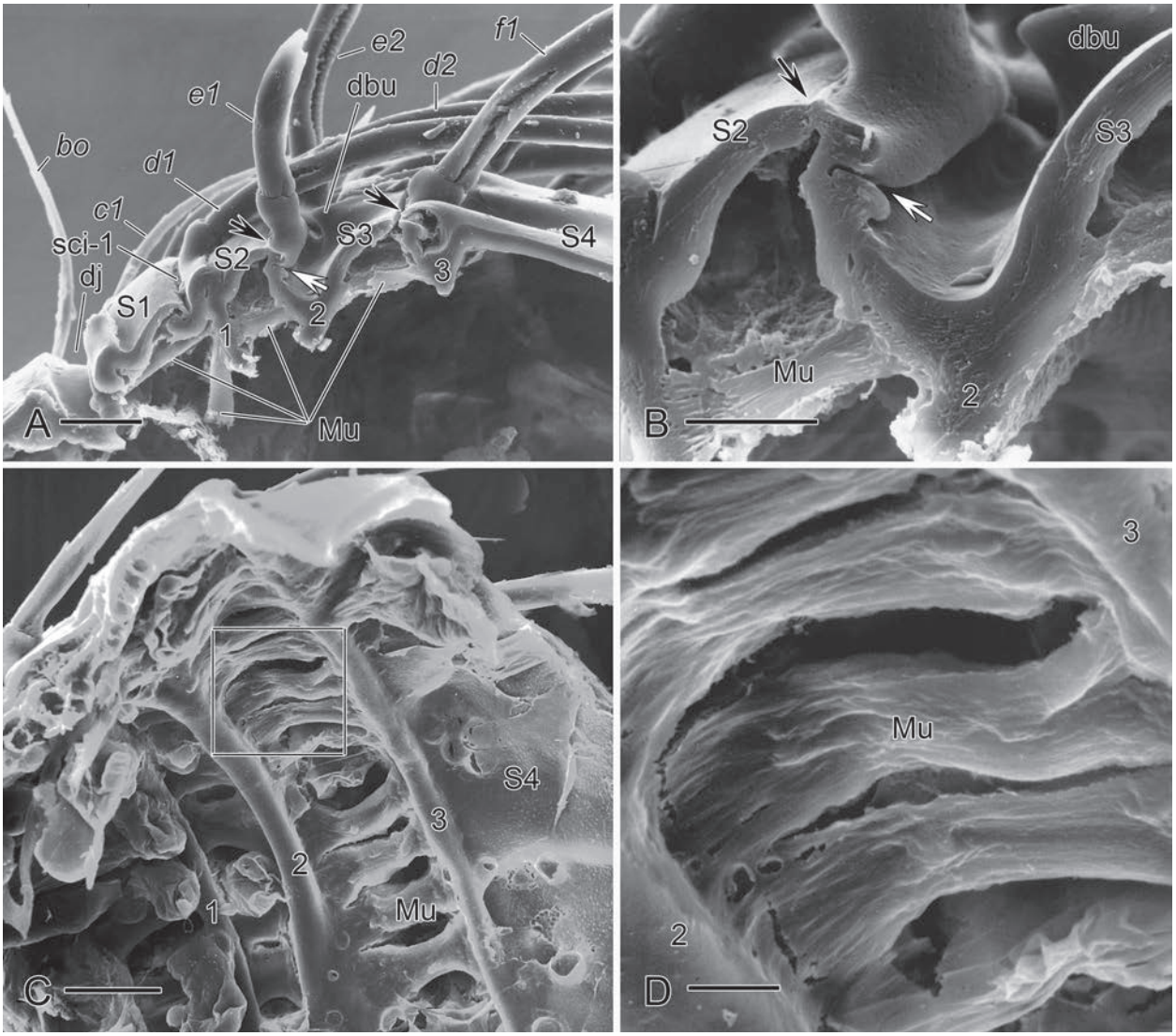

▲ **Figure 3**. SEM-figures of dissected *Heterochthonius gibbus* specimens (**A**) View on anterior notogaster of specimen cut in sagittal plane. Note apodemal ribs (1-3) and muscles connecting them. Note that setae *e2* and *f1* are partly cut open. Black arrows point to thin line of flexibility in front of setal rows *e* and *f* (that in front of row *f* is broken), white arrow indicates flexibility behind seta row *e* (= posterior border of intercalary sclerite). Scale bar: 25 µm. (**B**) Detail of Fig. 3A in higher magnification. Black, white arrows indicate the same as in Fig. A. Note that the muscles do not insert directly on the setal base. Scale bar: 10 µm. (**C**) Part of notogaster seen from its inner side. Note apodemal ribs (1-3) and muscles between them. Note that muscle arrangement in front of the anterior rib (at left) is much more complex than posterior to it. Squared area is shown in Fig. 3D. Scale bar: 25 µm. (**D**) Squared area of Fig. 3C in higher magnification. Muscles connecting two posterior apodemal ribs (2, 3). Scale bar: 5 µm.

Abbr.: **1-3** – apodemal ribs, ***bo*** – bothridial seta (trichobothrium), ***c1*** – seta of row *c*, ***d1, d2*** – setae of row *d*, **dbu** – dorsal bump, **dj** – dorsosejugal furrow, ***e1, e2*** – erectile setae of row *e*, ***f1*** – erectile seta of row *f*, **Mu** – muscles, **S1-S4** – sclerites 1-4, **sci-1** – scissure 1.

are not parts of the glands. The microvilli may extend against the cuticle of the notogaster, which is not modified above these microvilli.

Sclerites, apodemes and muscles: In sagittal sections approaching the median axis of the mite, the anterior borders of the sclerites 2, 3, and 4 project into the body as transversal apodemal ribs (Figs 7, 8) to which muscles attach reaching between ribs 1 and 2 and 2 and 3, thus paralleling the longitudinal axis of the mite (Figs 3A–C, 7, 8). Whereas ribs 2 and 3 are slightly bent anteriorly when transversely sectioned, rib 1 extends more vertically and also deeper into the body. It serves on its anterior side as origin for a muscle that inserts on a thin cuticular lamella that extends from the posterior and ventral border of the dorsosejugal furrow deeply into the body (Figs 7G–H). A similar muscle is located more dorsal of the latter one and spans between the thick cuticle located just behind scissure 1 and the thin lamella. Contraction of this muscle may erect the setal row *d* to some degree (Fig. 7F–H). The fine structure of these muscles differs remarkably. The two muscles inserting on the small lamella ventral of the dorsosejugal furrow comprise two or three sarcomeres with distinct Z-bands. However, the muscles stretching between ribs 1 and 2 and 2 and 3 present only one (peculiar) sarcomere each (Figs 8A, D, 9A, B). They are thus non-striated muscles, although the arrangement of myofilaments is very regular and dense, quite different from typical smooth muscles (compare

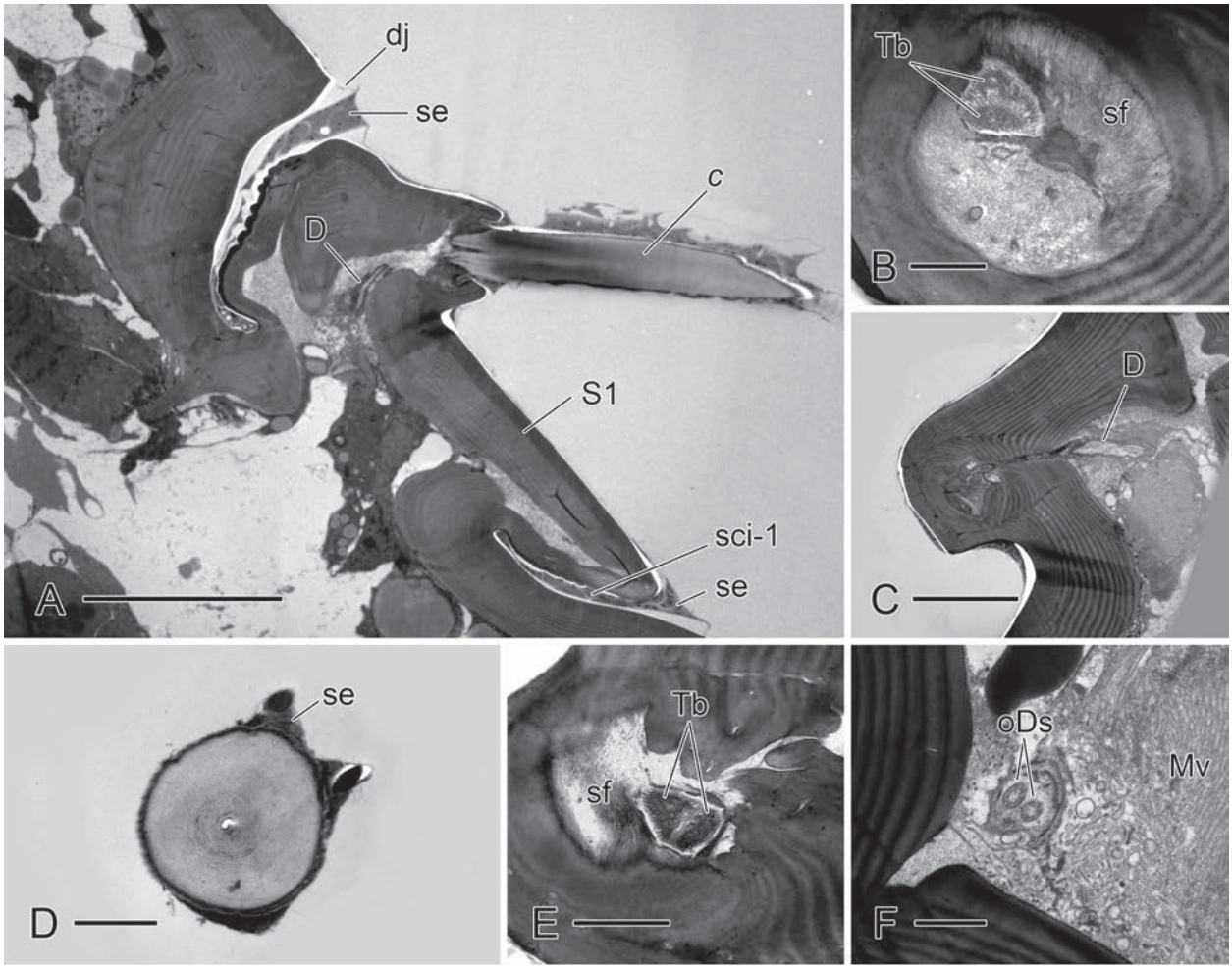

▲ **Figure 4**. TEM-figures of notogastral setae of *Heterochthonius gibbus*. (**A**) Seta of *c*-row. Note that the seta is mostly solid showing only small cavity in its basal part. Accumulations of secretions are visible in the dorsosejugal furrow and in scissure 1. Note fine ripples in cuticle of the posterior border of the dorsosejugal furrow and thin flexible cuticle in that area. Note also the slight overlapping of sclerite 1 over scissure 1, which resembles a small tectum. Scale bar: 10 µm. (**B**) At the base of a seta of row *c*, two tubular bodies contact the suspension fibers of the seta. Scale bar: 1 µm. (**C**) Dendrites leaving the elevation on which a *c*-seta is located. Scale bar: 5 µm. (**D**) Transversal section of a *c*-seta. Note its solid structure with electron-lucent cuticle dominating. In the center a fine dense strand of different structure is sectioned and at the periphery the seta is covered by secretion. Scale bar: 1 µm. (**E**) Tiny seta *c3* is innervated by two tubular bodies, like large setae. Scale bar: 1 µm. (**F**) Outer dendritic segments of the two dendrites of a *c3*-seta. Note numerous long microvilli of adjacent auxiliary cell. Scale bar: 1 µm.

Abbr.: ***c*** – seta of row *c*, **D** – dendrite, **dj** – dorsosejugal furrow, **Mv** – microvilli, **oDs** – outer dendritic segment, **S1** – sclerite 1, **sci-1** – scissure 1, **se** – secretion, **sf** – suspension fibers, **Tb** – tubular body.

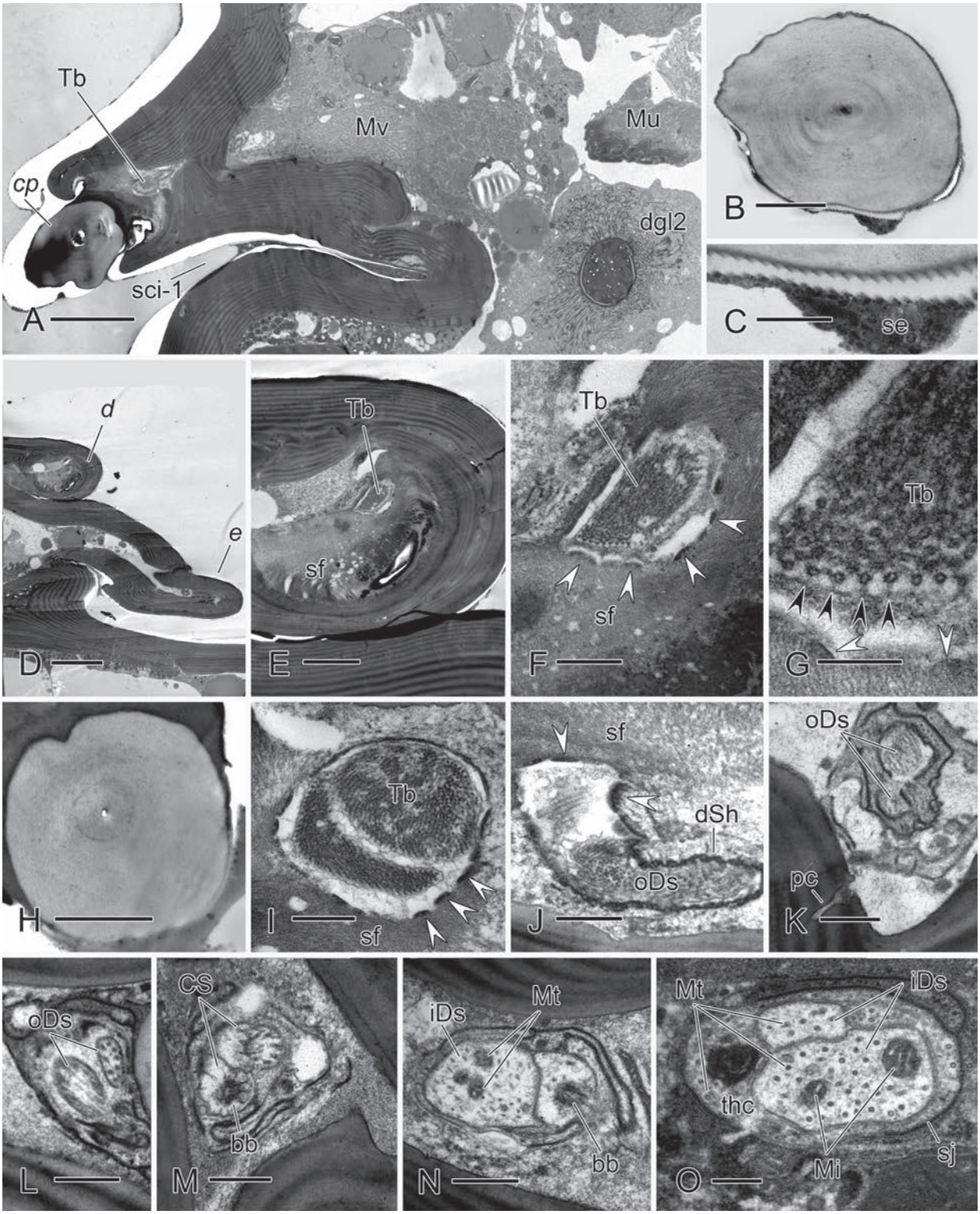

▲ **Figure 5**. Details of setae *cp* (A, B), *d* (F–F) and *e* (G–O). (**A**) Overview of insertion of seta *cp* in its flexible socket. Note small channel reaching into the base of the seta and tubular bodies attaching the suspension fibers. A dermal gland is located underneath scissure 1. Scale bar: 5 µm. (**B**) A more distal cross section through seta *cp* mostly composed of electron-lucent cuticle. Scale bar: 2 µm. (**C**) Detail of preceding figure showing the slightly rippled surface covered by secretion (partly removed artificially). Scale bar: 0.5 µm. (**D**) Overview showing insertion sites of setae *d* and *e* (horizontal section). Scale bar: 10 µm. (**E**) Close up of preceding figure with a tubular body reaching the suspension fibers of seta *d*. Scale bar: 2 µm. (**F**) The same tubular body of seta *e* in higher magnification. Note the half-round densities close to the suspension fibers (white arrowheads). Scale bar: 0.5 µm. (**G**) Detail of the tubular body showing microtubules connected to the cell membrane of the dendrite by tiny dense bars (black arrowheads). White arrowheads point to half-round densities, to which the ...

Fig. 9B, C). It seems remarkable that M- and H- bands were not obvious in these muscles and also tubules were rarely seen. Mitochondria are located mainly in the periphery where also the nucleus is positioned (Fig. 9D). The muscles attach to the apodemes via tendon cells, specialized epithelial cells that contain numerous microtubules. The desmosomes connecting the tendon cell with the muscle cell are arranged in a zig-zag pattern (in section). Numerous electron-dense tendon fibers are formed from extracellular material that indent the tendon cells, but extend also into the apodemal cuticle. Similar non-striated muscle cells were also observed in eriophyoid mites (Alberti & Nuzzaci 1996b, Alberti & Coons 1999).

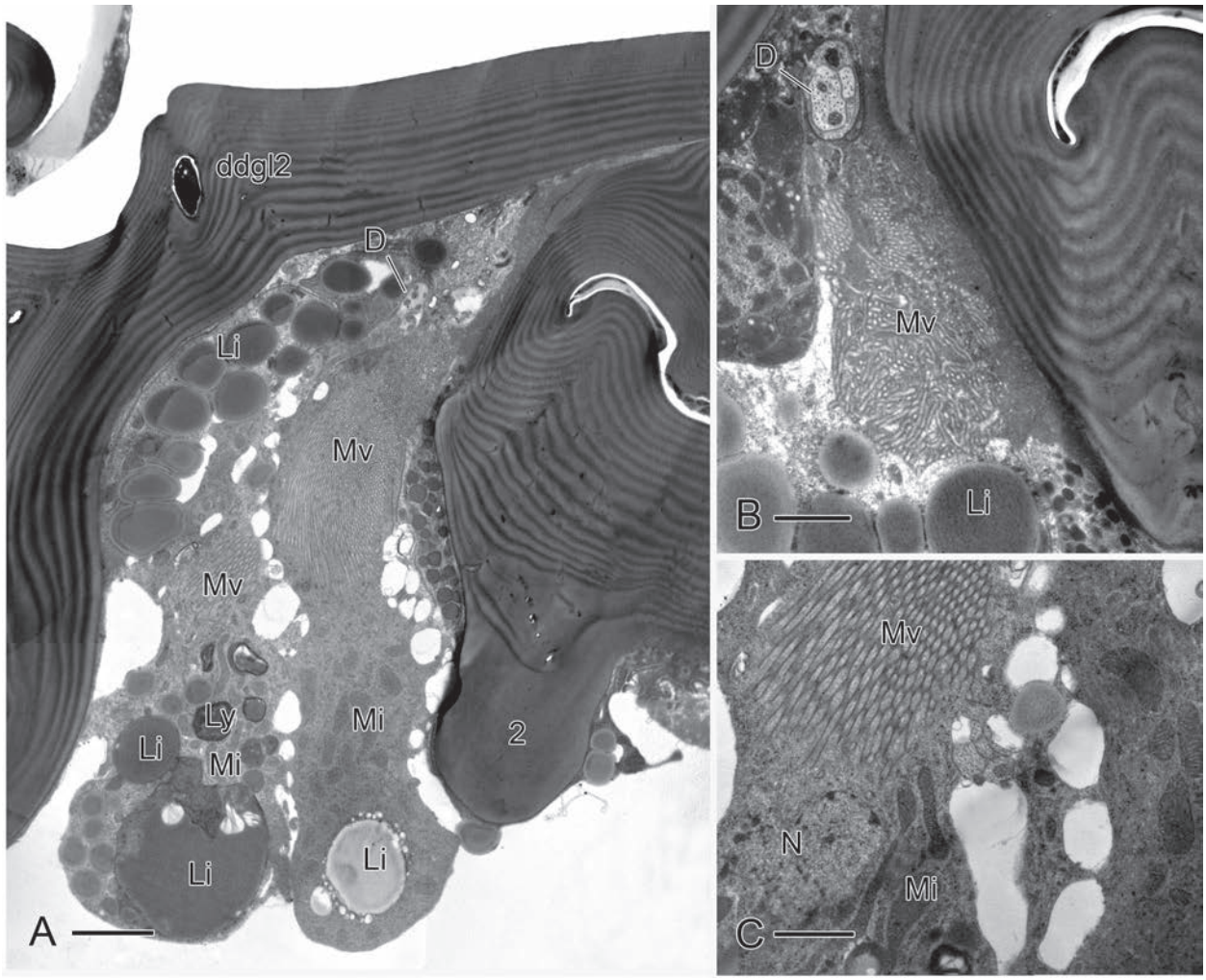

▲**Figure 6**. Auxiliary (i.e. trichogen, tormogen) cells of a seta *d*. (**A**) Overview showing the two auxiliary cells containing numerous lipid inclusions and the hardly visible dendrites of a seta of the *d*-row. Note canal of dermal gland 2. Scale bar: 2 µm. (**B**) Dendrites of a *d*-seta and adjacent microvilli of an auxiliary cell extending against the cuticle. Scale bar: 1 µm. (**C**) The nucleus is located underneath the long, parallel microvilli. Scale bar: 1 µm.

Abbr.: **2** – apodemal rib 2, **D** – dendrite, **ddgl2** – duct of dermal gland 2, **Li** – lipid inclusion, **Ly** – lysosome, **Mi** – mitochondrium, **Mv** – microvilli, N – nucleus.

(◄ continued figure 5) suspension fibers attach. Scale bar: 0.2 µm. (**H**) Cross section through seta *e* close to its insertion. Note that it is almost completely made of electron-lucent cuticle and that it is a massive structure. Only a tiny central densitiy is visible. Scale bar: 2 µm. (**I**) The two tubular bodies at the base of a seta *e*. White arrowheads indicate half-round densities. Scale bar: 0.5 µm. (**J**) The half-round densities continue into a thin dendritic sheath that surrounds the outer dendritic segments. Scale bar: 0.5 µm. (**K**) More proximally the dendritic sheath disintegrates into irregular sheets. Scale bar: 0.5 µm. (**L**) Closer to the proximal end of the outer segment of the dendrite the microtubules form a cilium-like pattern. Scale bar: 0.5 µm. (**M**) The ciliary segment with basal bodies. Scale bar: 0.5 µm. (**N**) The inner dendritic segment in cross section is wider and contains mitochondria. Scale bar: 0.5µm. (**O**) Inner segments in higher magnification. The thecogen cell closely ensheathes the dendrites. Scale bar: 0.2 µm.

Abbr.: **bb** – basal body, ***cp*** – seta *cp*, **CS** – ciliary segment, ***d*** – (insertion of) seta *d*, **dgl2** – dermal gland 2, **dSh** – dendritic sheath, ***e*** – (insertion of) seta *e*, **iDs** – inner dendritic segment, **Mi** – mitochondrium, **Mt** – microtubule, **Mu** – muscle, **Mv** – microvilli, **oDs** – outer dendritic segment, **pc** – pore canal, **sci-1** – scissure 1, **se** – secretion, **sf** – suspension fibers, **sj** – septate junction, **Tb** – tubular body, **thc** – thecogen cell.

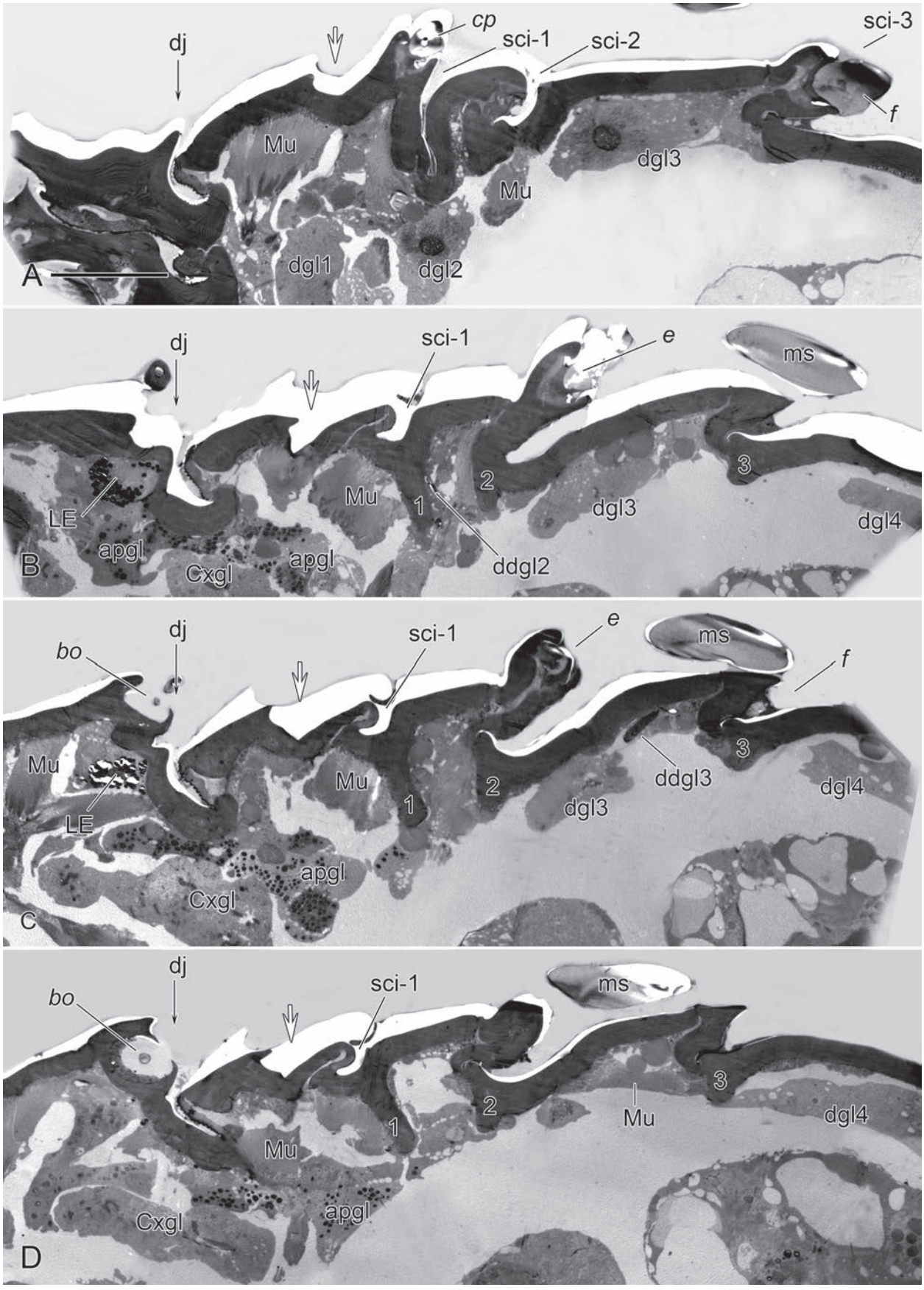
dj
cp
sci-1
sci-2
sci-3
f
Mu
dgl3
Mu
dgl1
dgl2
A
dj
sci-1
e
ms
3
2
Mu
1
dgl3
dgl4
LE
apgl
Cxgl
apgl
ddgl2
B
dj
bo
sci-1
e
ms
f
Mu
3
Mu
2
ddgl3
dgl4
1
dgl3
LE
apgl
Cxgl
C
dj
bo
sci-1
ms
3
2
Mu
dgl4
1
Mu
apgl
Cxgl
D

Muscles originating on the anterior sides of the cuticle of the dorsosejugal furrow and its thin lamella run anteroventrad and are not considered further here.

There is a region at the bottom of the dorsosejugal furrow where the cuticle is thin and thus likely flexible so that the proterosoma can slightly be moved (bent or protruded and retracted) against the hysterosoma due to contraction of the two muscles mentioned above. The cuticle in this area, bordering the dorsosejugal furrow posteriorly, is peripherally finely rippled (Figs 2C, 4A, 7). This may allow the epicuticle, which probably cannot be stretched (Alberti et al. 1981, Alberti & Coons 1999, Coons & Alberti 1999), to follow these movements.

The transversal sclerites posterior of the dorsosejugal furrow overlap each other with their posterior borders as mentioned above. The sclerite 3 is flexibly joined with the sclerite 2 (scissure 2) and the posterior sclerite 4 (undivided posterior notogaster; scissure 3) by specialized cuticle. These flexibilities are thus just positioned behind the setal rows *e* and *f* (Fig. 7). No such flexible cuticle was found in the sclerite 2 behind setal row *d*. Instead, a flexibility is present in the cuticle just in front of setae *d* (representing scissure 1). All setae under concern are inserted into a flexible socket, so that they can be moved passively (Figs 4A, 5A, 7A–C, G, H, 8A, E, F, 9A).

The rows *e* and *f* of erectile setae show the peculiarity that they are inserted on so-called intercalary sclerites, which need a closer look. These structures are hard to recognize and understand at a first glance in the sections. Their posterior border is evident and located deep in the fold posterior of a setal row. There is a flexible cuticle as is typically found joining two sclerites (Figs 7, 8). On the contrary, just in front of the setae, a very fine slit in the procuticle is visible (Fig. 8), which corresponds with the thin line observed in the SEM (Fig. 2D–G) in front of the setae. This peculiar slit obviously provides an additional flexible region in the cuticle of the sclerite and presents the anterior border of the intercalary sclerites. Remarkably, such a slit in the procuticle is not found in front of setal row *d* (Figs 7G, H, 8A).

Glands: We observed rather conspicuous paired glands that are associated with the transversal sclerites. We could distinguish four pairs but could detect only three pairs of pores in our SEM-figures and failed yet to find the pores of the most anterior pair of glands. The pores and distal ducts are very small or thin and are often hidden by the overhanging thick setae or the overlapping sclerites (Figs 2, 8D, 10C, 12). The anterior glands are located dorsolaterally above and lateral of the coxal glands. The body of the anterior dermal gland is located underneath the first sclerite, the second is found slightly more posterior, approximately underneath the first scissure. The next one is positioned underneath sclerite 3 and the last and probably largest one is located under sclerite 4 behind setal row *f* (Figs 7A–F, 10A–C).

These glands are rather similar in structure. They are proximally composed of at least four rather large cells that contain numerous Golgi bodies, which consist of electron lucent cisternae and vesicles. The lucent vesicles probably fuse to form large 'empty' inclusions (Fig. 11A, B). Large nuclei are present with finely dispersed spots of heterochromatin and a distinct nucleolus. The cells are connected by long, electron-dense septate junctions (Figs 10E, 11C, D, H). Dense secretion is formed by the granular ER- and ribosome-rich cytoplasm. These secretions are extruded via small vesicles into a lumen that is largely occupied by irregularly arranged apical cell protrusions that extend into undulating microvilli (Figs 11, 12A). The apical regions of the cells contain many microtubules (Fig. 11E).

However, in some sections we also observed bundles of parallel and tightly packed microvilli, which make these cells sometimes difficult to distinguish from those belonging to the auxiliary cells of the setal complexes (compare Fig. 6C and Fig. 10D). We think that this different appearance of cell apices is a consequence of different filling states of the reservoirs, since the parallel and tightly arranged microvilli were correlated with the cogwheel shape of the reservoir (Fig. 10B, D, E). This peculiar shape apparently represents a gland that is more or less emptied. More frequently we observed glands with a roundish reservoir and with the irregular arrangement of microvilli and apical cell protrusions. The mainly dense secretion is filling the spaces between the protrusions and microvilli and is more distally collected in a roundish reservoir provided with a thin cuticle (Fig. 11B–D, F). The secretion within the reservoir is very distinct being composed of many dense granules embedded in a less dense matrix. Some more electron-transparent spheres are also found. Their contents often get lost artificially during sectioning. The secretion forms quite regular 'compartments'. From this reservoir region, a duct starts that becomes thinner and thinner towards its distal end. The duct also may be squeezed or flattened (Fig. 12E, F). It is proximally surrounded by a rather thick layer of cells with granular cytoplasm containing rather large nuclei

◄ **Figure 7**. Sequence of sagittal sections (A–D) through periphery of anterior notogaster level with the lateral eye and bothridial seta. White arrows indicate transversal depression behind seta row *c*. All figures to the same scale as shown in Fig. A. Scale bar: 20 µm.

Abbr.: **1-3** – apodemal ribs 1-3, **apgl** – acinous podocephalic gland, ***bo*** – bothridial seta (trichobothrium), ***c*** – seta of row *c*, ***cp*** – seta *cp*, **Cxgl** – coxal gland, *d* – seta of row *d*, **dgl1-4** – dermal glands 1-4, **ddgl2-4** – ducts of dermal glands 2-4, **dj** – dorsosejugal furrow, ***e*** – erectile seta of row *e*, ***f*** – erectile seta of row *f*; **LE** – lateral eye, **ms** – (undetermined) macroseta, **Mu** – muscle, **sci-1** – scissure 1, **sci-2** – scissure 2, **sci-3** – scissure 3.

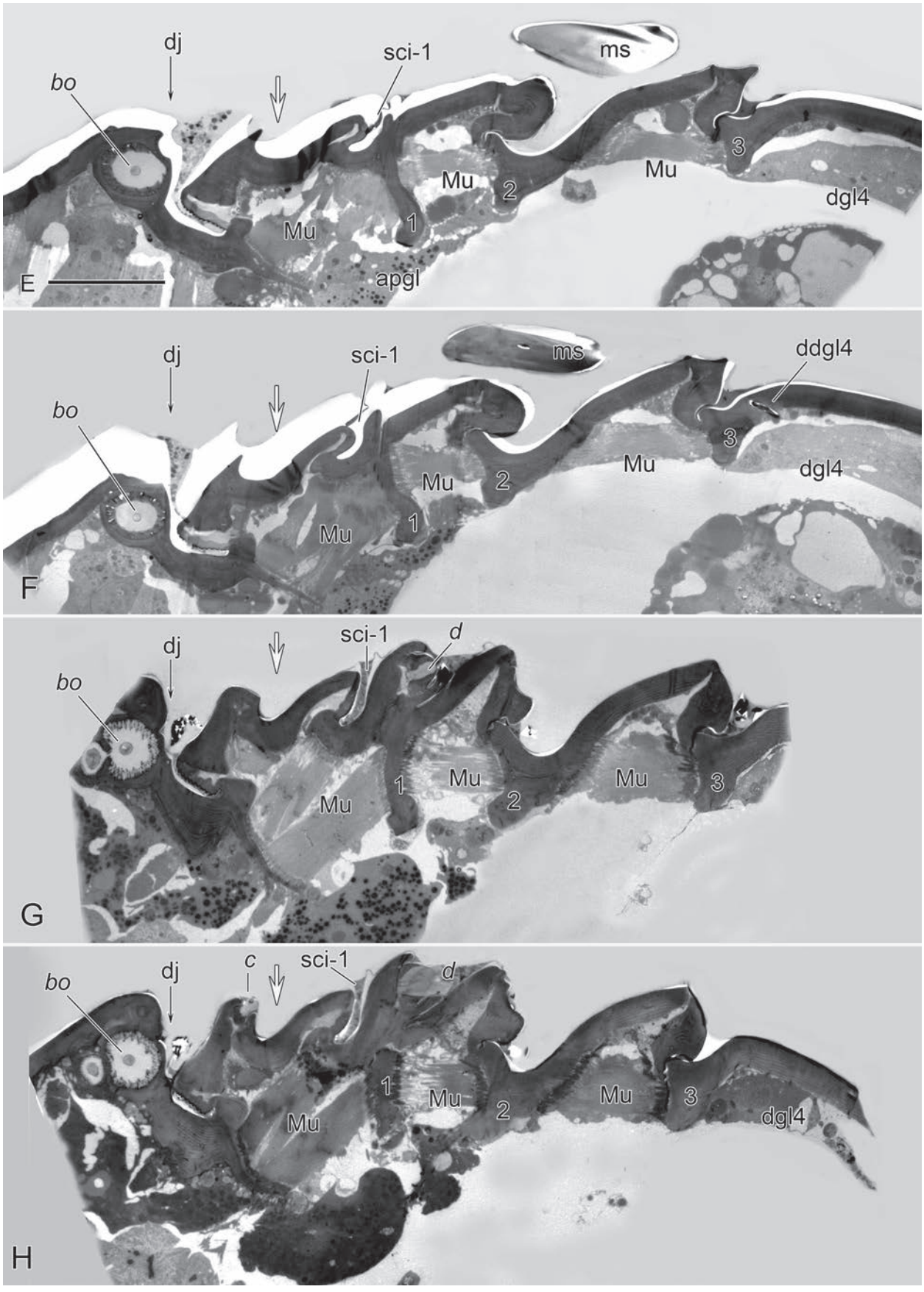
dj
sci-1
ms
bo
3
Mu
Mu
2
dgl4
Mu
1
E
apgl
dj
sci-1
ms
ddgl4
bo
3
Mu
dgl4
Mu
2
Mu
1
F
dj
sci-1
d
bo
Mu
1
Mu
2
Mu
3
G
c
dj
sci-1
d
bo
1
Mu
Mu
2
Mu
3
dgl4
H

and a diversity of lipid and lysosomal inclusions (Figs 12A, B). These cells do not have microvilli (Fig. 12A–E). Finally the duct enters the cuticle of the body surface. About half of the procuticle the epithelial layer ends and the duct opens into a rather deep, tubular indentation of the cuticle. The secretion is delivered into this tube, and finally spreads over the cuticle of the body surface (Figs 6A, 12D–I). Since the secretion shows the typical granular fine structure, it can be recognized as a thin film on the body surface or in higher amounts in depressions like the sockets of setae (Figs 4A, C, D, 8C, E, F, 10C, 12I).

We did not find any muscle layer underneath the glandular epithelium. Sometimes we observed small nerves (Fig. 11H), but could not decide whether the glands are really innervated.

Finally, it should be stated that these glands do certainly not belong to the podocephalic system, which is represented by the paired tubular coxal glands and the acinous glands composed of cells full of dense granules (Figs 7B–H).

4. Conclusions

The present study revealed some unexpected peculiarities in these remarkable oribatid mites.

However, first of all we can suggest a functional model for the movements of the setae. According to our observations, the intercalary sclerites are formed by the specialized posterior borders of the broad sclerites 2 and 3. Our suggestion is that these sclerites are separated from the posterior ones by scissures which might have evolved from type L scissures provided with a tectum on which the setae have been transferred. These tecta have an (additional, and probably secondary) flexible region slightly in front of their setae, this region being a slit in the procuticle is evident as a thin line in the SEM-figures. Thus, when the muscles connecting the apodemal transversal ribs are contracted, the cuticle is bent in such a way that the setae become erect (see Fig. 13A). By small posterior indentations or incisions with flexible cuticle between the setae, the interacalary sclerites are formed, which allow a lateral spreading of the setae *e* and *f*. When the muscles relax, the setae *e* and *f* are laid down passively on the notogaster due to the stiffness of the cuticle in front of the setae. Thus we are in accord with the suggestion of Grandjean (1931) that the movements of the setae are based on an indirect mechanism. But we deviate from Grandjean′s (1931) point of view in suggesting that at least in this species the erection occurs due to a contraction rather than due to a dilation of the hysterosoma. We think that our interpretation with the peculiar muscles forcing the erection is more plausible than the alternative suggested by Norton & Fuangarworn (2015) for *Nanohystrix hammerae* that the muscles are used to lay the setae down. We think that the activity of muscles would allow a quicker answer against an irritation than an indirect force created by alteration of internal hydrostatic pressure. Also, if the muscles would be involved in keeping the setae close to the body, they would be more or less permanent in action and thus more energy costy. However, we admit that the movements of setae may be different in those taxa provided with this capability (Norton 2001). This capability of setal movement is found in a number of early derivative oribatid mites and has been considered a plesiomorphy of these mites (Norton 2001, Weigmann 2001, Norton & Behan-Pelletier 2009, Norton & Fuangarworn 2015).

During our study which was first focused on the erectile setae only, we found dermal glands for the first time in Enarthronota.

In Oribatida dermal glands may generally be classified into two categories: 1. A pair of lateral opisthosomal (opisthonotal, lateroabdominal, oil) glands (e.g., Norton 1998, Norton & Behan-Pelletier 2009). 2. Secretory porose areas and their derivatives (e.g., saccules, vesicles, tubules) distributed on various places of the body of the mites (e.g., Alberti et al. 1997, Alberti & Coons 1999).

Considering the first category, the detection of rather conspicuous dermal glands in a species belonging to Enarthronota is very remarkable since such dermal glands until now were thought to occur only in the so-called glandulate Oribatida (i.e. Parhyposomata, Mixonomata, Desmonomata with Brachypylina; Norton 1998) possessing one pair of large opisthonotal glands. These glands produce complex secretions that are used for different purposes: as aggregations/alarm/sex pheromones or as defense substances against predators (Krantz 2009, Norton & Behan-Pelletier 2009). Interestingly, these glands are among other characters mentioned as a synapomorphy connecting these mites, in particular the oribatid subgroup Desmonomata, with Astigmata (= Acaridida, Astigmatina), which are now regarded as part of the Oribatida (s.l.; e.g., Norton 1998, Raspotnig 2006, Norton & Behan-Pelletier 2009,

(◄ continued figure 7) Sequence of sagittal sections (E–H) through periphery of anterior notogaster level with the lateral eye and bothridial seta. White arrows indicate transversal depression behind seta row *c*. All figures to the same scale as shown in Fig. E. Scale bar: 20 µm.

Abbr.: **1-3** – apodemal ribs 1-3, **apgl** – acinous podocephalic gland, ***bo*** – bothridial seta (trichobothrium), ***c*** – seta of row *c*, ***cp*** – seta *cp*, **Cxgl** – coxal gland, *d* – seta of row *d*, **dgl1-4** – dermal glands 1-4, **ddgl2-4** – ducts of dermal glands 2-4, **dj** – dorsosejugal furrow, ***e*** – erectile seta of row *e*, ***f*** – erectile seta of row *f*; **LE** – lateral eye, **ms** – (undetermined) macroseta, **Mu** – muscle, **sci-1** – scissure 1, **sci-2** – scissure 2, **sci-3** – scissure 3.

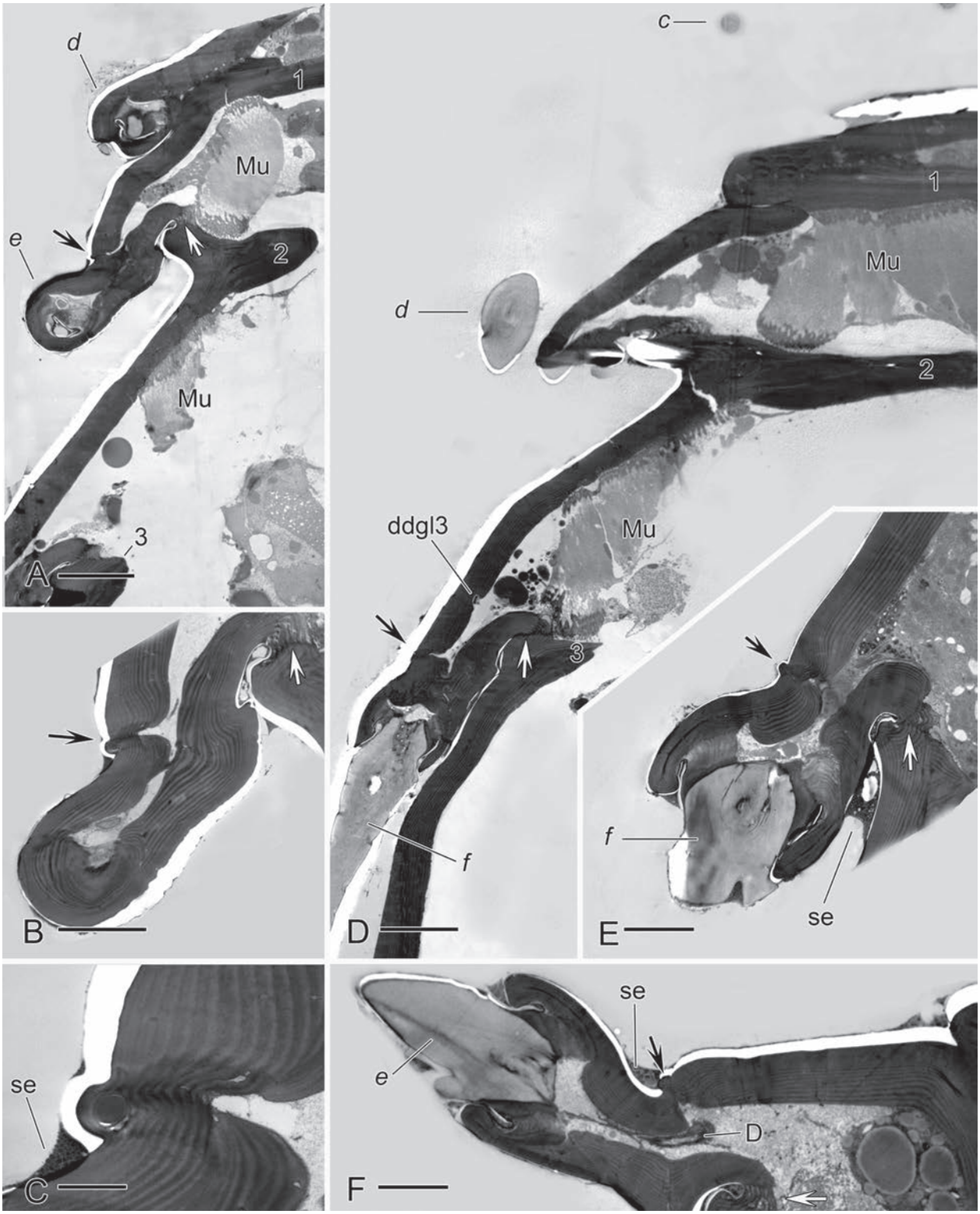

▲ **Figure 8**. Horizontal (A–C, E) and sagittal sections (D, F) showing the insertion of setae *d*, *e* and *f*. Black arrows indicate thin flexible line in front of setae *e*, *f* (= anterior border of intercalary sclerite). White arrow marks flexible scissure behind row *e*, *f* (= posterior border of intercalary sclerite). (**A**) Overview showing insertion of a seta *d* and a seta *e*. Note that the bulge bearing seta *d* lacks the flexible regions indicated for seta *e* by arrows. The intercalary sclerite of seta *e* is slightly erected. Scale bar: 10 µm. (**B**) An intercalary sclerite of seta row *e* with its flexible borders demarcated by arrows. Scale bar: 5 µm. (**C**) The flexible anterior border of the intercalary sclerite of row *e* in higher magnification. Note that the procuticle is much thinner due to a deep proximal slit and the cuticle above the slit is deformed. Scale bar: 1 µm. (**D**) Overview showing about half of the anterior notogaster sectioned more dorsally than in Fig. 8A. The apodemal ribs are connected by muscles. Note intercalary sclerite bearing a seta of row *f* with its borders demarcated by arrows. The seta is in a not-erected position and ...

OConnor 2009, Dabert et al. 2010). Further studies are needed to clarify the character state of the newly detected glands, which occur in a higher number and in different structure in *Heterochthonius gibbus* than in the glandulate Oribatida s. l. (e.g., Alberti & Coons 1999, Raspotnig et al. 2003, 2009). In any case, the close spatial relationship of these glands with the large setae, which in part are evidently used as defense structures, may suggest that the glands of *H. gibbus* also provide a defensive secretion, which might be pushed outward and spread over the body surface when the mentioned muscles contract and the setae are erected. Thus, the idea that the more evolved Oribatida have reduced the number of dermal glands to one pair is attractive. But to support this, an investigation of other Enarthronota with regard to dermal glands is evidently necessary.

Regarding the second category of dermal glands, the large microvilli-cells are rather peculiar. These cells very much resemble the cells forming the various structures termed secretory porose areas in oribatid mites (see Alberti et al. 1997). But in contrast to these porose areas which are considered to participate at least in part in cerotegument formation, we could not detect any modification in the cuticle above these cells. It is not thinner than surrounding areas, nor does it show thicker or more abundant pore canals. No signs of any secretion delivered from these cells were observed. At present we think that these very large microvilli-cells represent (extraordinary) large trichogen and tormogen cells. Nevertheless the similarity of these cells with those forming the porose areas seems remarkable. Norton & Alberti (1997) interestingly suggested that the cells forming the (secretory) porose areas likely evolved from secretory cells at the base of setae! In the mentioned *Nanohystrix hammerae*, Norton & Fuangarworn (2015) described areas which resembled porose areas. But no signs of dermal glands were observed in this new species. On the contrary, the detailed study on *Collohmannia johnstoni* by Norton & Sidorchuk (2014) stated a close association of porose areas and setae.

In many of the so-called higher Oribatida (Brachypylina), the porose areas on the notogaster are arranged as four pairs comprising the octotaxic system, a characteristic that is used for long time for taxonomical purposes (e.g., Norton et al. 1997, Weigmann 2006, Norton & Behan-Pelletier 2009). Of course it is tentative to consider a relationship of this peculiar arrangement with the four pairs of dermal glands present in *H. gibbus*. But due to the facts just discussed we think that these glands of *H. gibbus* are not related to porose areas.

Nevertheless, at the moment three interpretations of the newly observed glands of *H. gibbus* may be considered: 1. The glands are homologous with the opisthonotal glands of glandulate Oribatida, which reduced the number of glands to one pair. 2. The glands are homologous with porose areas. 3. The glands are an autapomorphy of *H. gibbus*.

In any case more studies of enarthronote mites are necessary to clarify the state of these glands. The chemical analysis of the secretions produced by these glands may be helpful. It is evident that the statement in Norton (1998) 'There is no reason to believe that the (opisthonotal) gland was ancestral in Acariformes or that it ever existed in …Enarthronota or their ancestors' needs to be reconsidered.

Our study may also stimulate some further thinking about the segmental organization of the notogaster in these mites discussed extensively by Weigmann (2001). In short, the discussion is whether there is a further (reduced) segment included in segment C, the region represented by sclerite 1 bearing the setae *c* as suggested by Hammen (1963, 1989) or not (Weigmann 2001). This (reduced) segment could correspond with the setae *cp* according to the more traditional view, whereas Weigmann (2001) denying the existence of such a reduced segment regards these setae as belonging to the setal row *d* as part of segment D terming it thus *d3*. However, our results evidently show, that the region under concern, i.e. that below sclerite 1, corresponding to segment C, is at least much more complex than the areas under the following sclerites 2 and 3 (representing segments D, E and F). Furthermore it is evident from our figures that the setae under concern, i.e. *cp* (*d3*), are positioned distinctly separately from the (other) *d* setae on a small area of sclerite 1, bordered anteriorly by a distinct transversal depression and posteriorly by scissure 1. In any case, scissure 1 distinctly separates the setae under concern (*cp/d3*) from the following setal row *d* as was already shown in the drawing by Grandjean (1928). This row *d* on the other hand is placed on a rather narrow transversal strand of sclerotized cuticle just above the vertical apodemal rib mentioned above. All this gives the impression that indeed this region bearing setal rows *c* and *d* is posteriorly much compressed in the anterior-posterior direction and may hide an additional segment that lost the median setae leaving only the lateral *cp* setae. In the schematic drawing

(◄ continued figure 8) the cuticle at the anterior flexible border of the sclerite (black arrow) is not deformed. The duct of dermal gland 3 enters the cuticle in front of seta *f* (compare Fig. 12F). Scale bar: 10 µm. (**E**) An intercalary sclerite bearing a slightly erected seta *f*. Note cuticle deformation at the anterior flexible border of the sclerite (black arrow). Scale bar: 5 µm. (**F**) Another view of an intercalary sclerite bearing a slightly erected seta *e*. Note deformation of cuticle of the anterior flexible border of the sclerite (black arrow). Scale bar: 5 µm.

Abbr.: **1-3** – apodemal ribs 1-3, ***c*** – seta of row *c*, **D** – dendrite, ***d*** – seta of row *d*, **ddgl3** – duct of dermal gland 3, ***e*** – erectile seta of row *e*, ***f*** – erectile seta of row *f*, **Mu** – muscle, **se** – secretion.

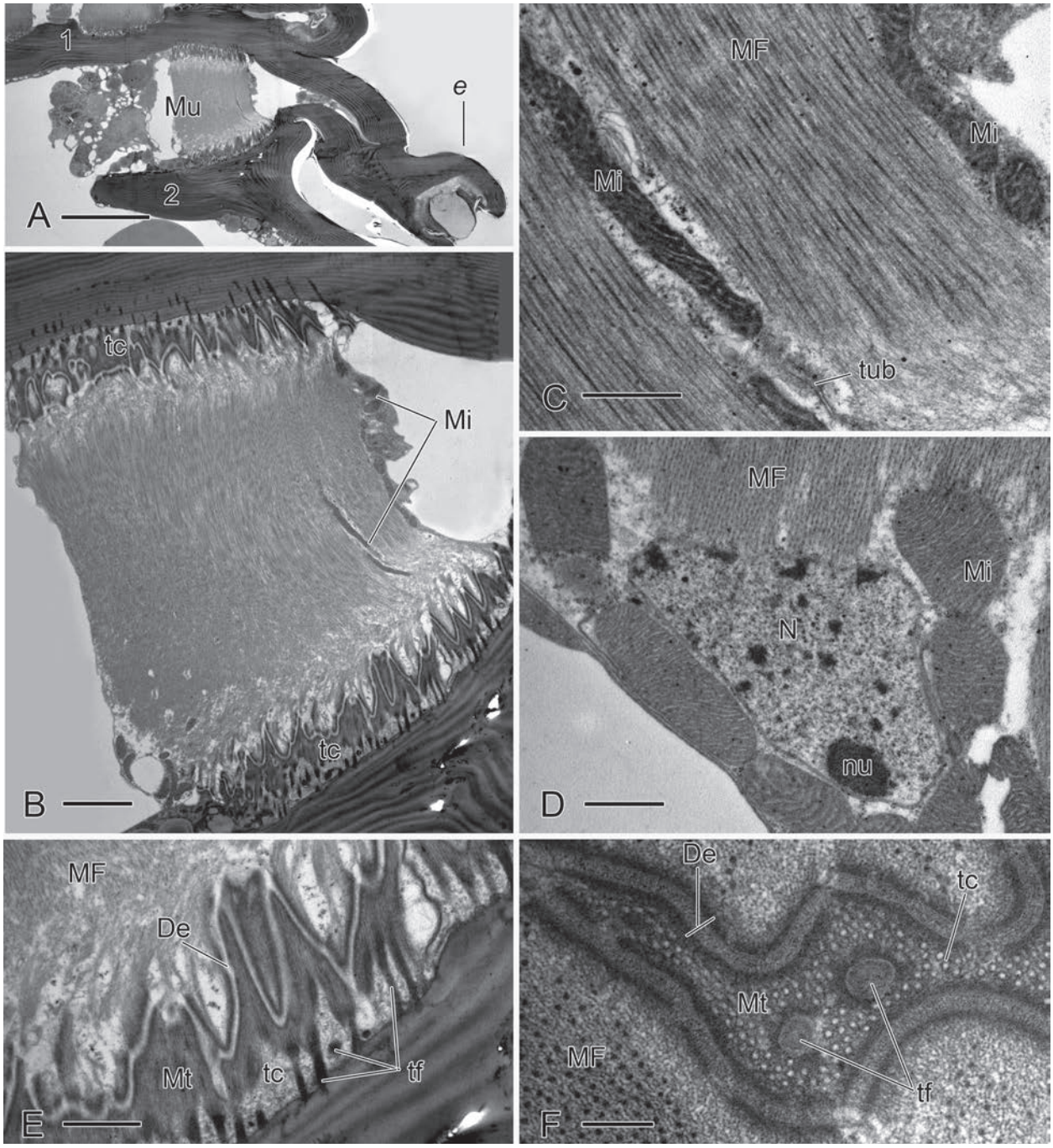

▲ **Figure 9**. Some details of the non-striated muscle cells connecting the apodemal ribs. Note that the cell shows neither Z-bands nor H- or M-bands. (**A**) Overview showing one muscle cell stretching between the apodemal ribs 1 and 2 bordering sclerite 2. Scale bar: 10 µm. (**B**) Same muscle in higher magnification. Note that the cytoplasm of the cell is densely filled with microfilaments (compare Fig. 9C). The muscle cell is connected with the apodemal ribs via tendon cells. Scale bar: 2 µm. (**C**) Detail of the same muscle cell showing densely arranged myofilaments (actin-, myosin filaments) and few mitochondria. One of the rare tubules (longitudinal or transversal tubule?) is also visible. Scale bar: 0.5 µm. (**D**) The nucleus is found together with rather large mitochondria in a peripheral position in the muscle cell. Scale bar: 1 µm. (**E**) Desmosomes connecting the muscle cell with the tendon cell show a zig-zag arrangement in the section paralleling the longitudinal axis of the muscle cell. Numerous microtubules are arranged in the tendon cell in the same orientation. Note that tendon fibers extend from the apodemal cuticle against the tendon cell. Scale bar: 1 µm. (**F**) A section through the desmosomes perpendicular to that shown in the previous figure 9E. Note abundance of microtubules in the tendon cell. Scale bar: 0.2 µm.

Abbr.: **1, 2** – apodemal ribs 1 and 2, **De** – desmosome, ***e*** – seta of row *e*, **MF** – myofilaments, **Mi** – mitochondrium, **Mt** – microtubules, **Mu** – muscle cell, **N** – nucleus, **nu** – nucleolus, **tc** – tendon cell, **tf** – tendon fibers, **tub** – part of the tubular system of the muscle cell.

► **Figure 10**. Dermal glands of *Heterochthonius gibbus*. (**A**) Quite lateral sagittal section showing position of dermal glands 1-3. Scale bar: 10 µm. (**B**) Slightly more medially, the reservoir of the anterior dermal gland 1 is sectioned (black arrow). Scale bar: 5 µm. (**C**) Sagittal section through dermal gland 4 level with its spherical reservoir (black arrow) and duct running into the cuticle. Scale bar: 10 µm. (**D**) Reservoir ...

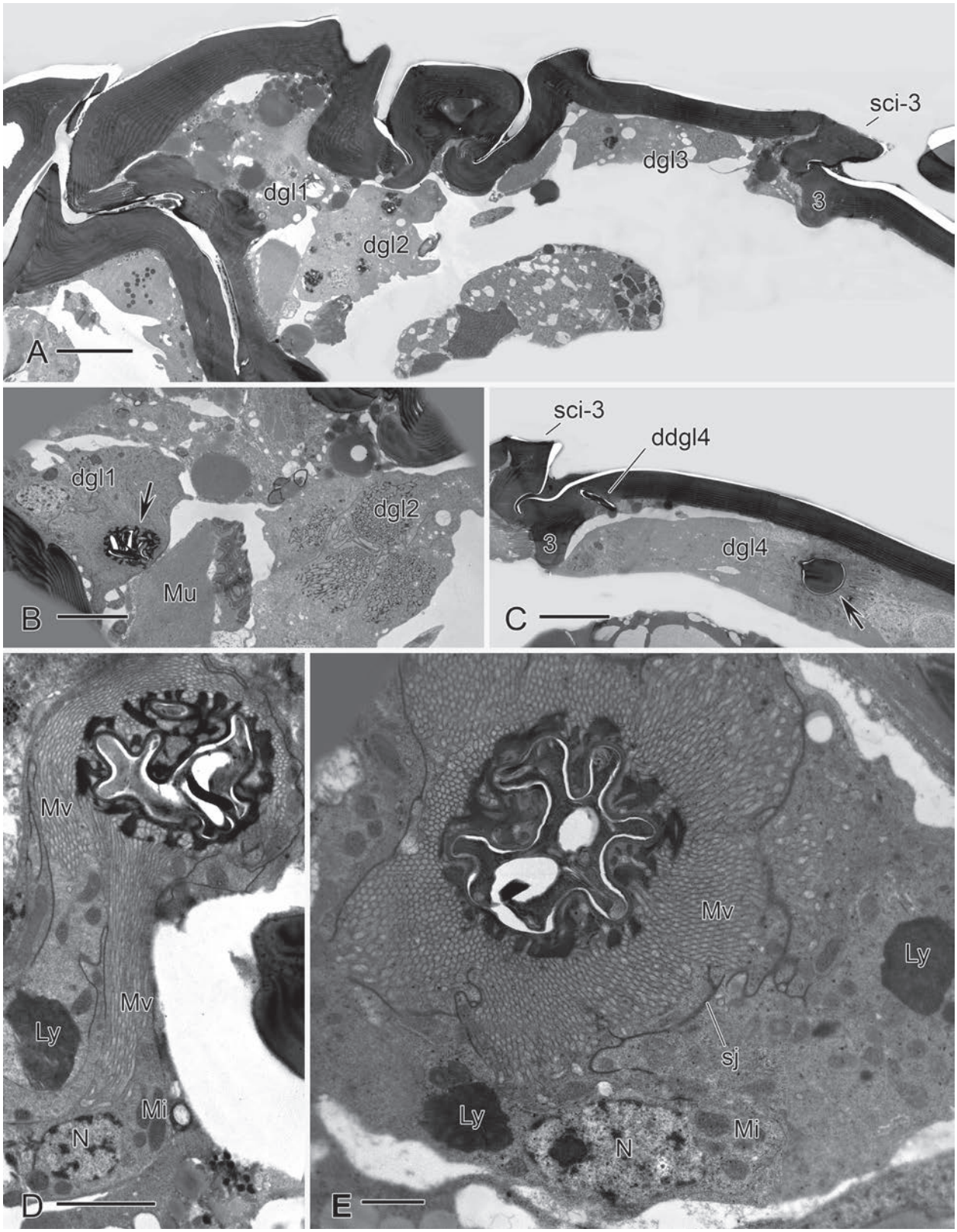

(▲ continued figure 10) of dermal gland 1 contracted and gland cells showing long and tightly packed parallel microvilli. Scale bar: 2 µm. (**E**) This section of a dermal gland 1 shows also the reservoir contracted giving it a cogwheel appearance and again the microvilli are arranged tightly together (compare Fig. 11). Scale bar: 1 µm.

Abbr.: **3** – apodemal rib 3, **dgl 1-4** – dermal glands 1-4, **ddgl4** – duct of dermal gland 4, **Ly** – lysosome, **Mi** – mitochondrium, **Mu** – muscle, **Mv** – microvilli, **N** – nucleus, sci-3 – scissure 3 (or intercalary sclerite of this scissure), **sj** – septate junction.

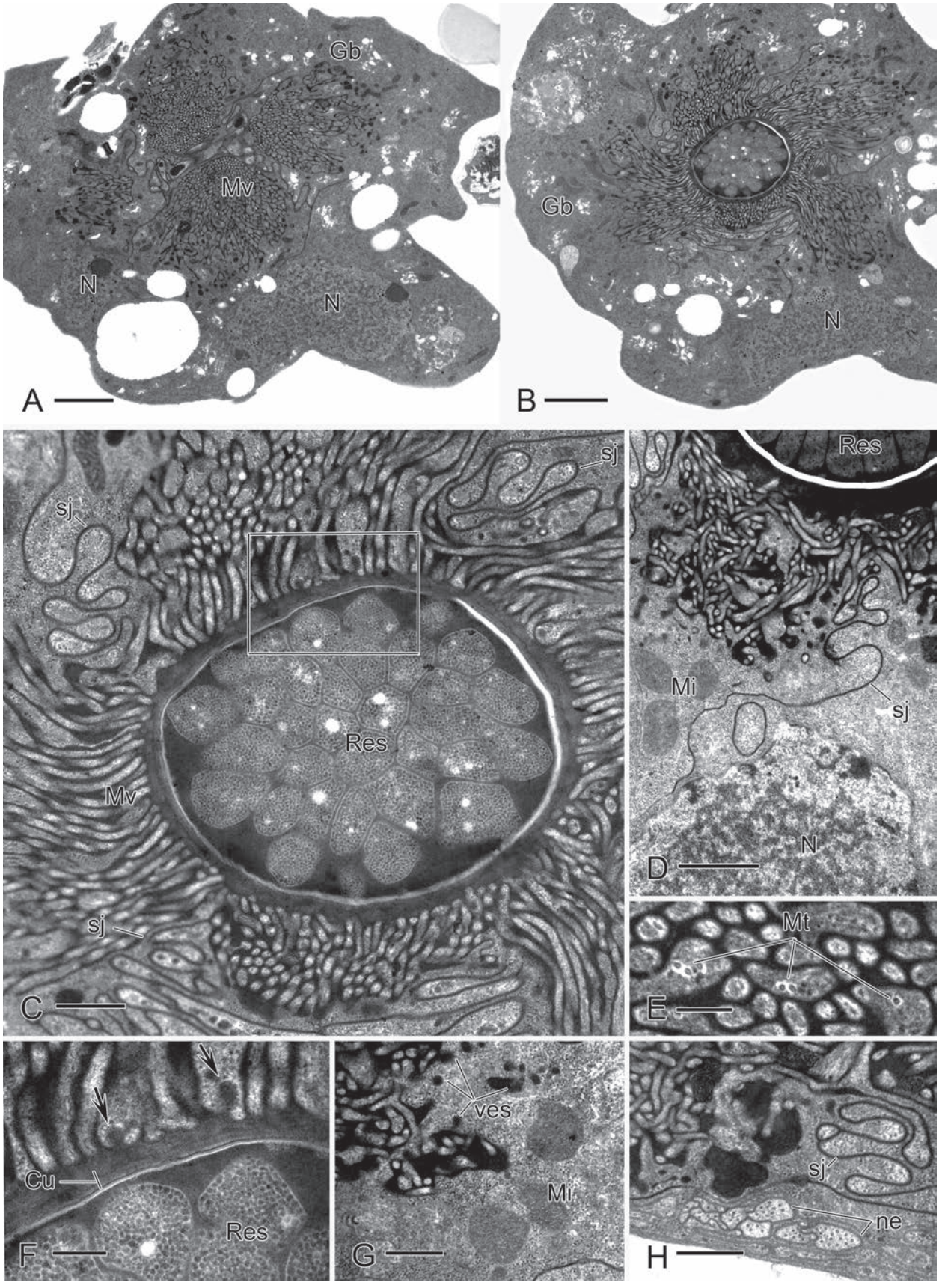
Gb
Mv
N
N
A
Gb
N
B
sj
sj
Res
Mv
sj
C
Res
Mi
sj
N
D
Mt
E
Cu
Res
F
ves
Mi
G
sj
ne
H

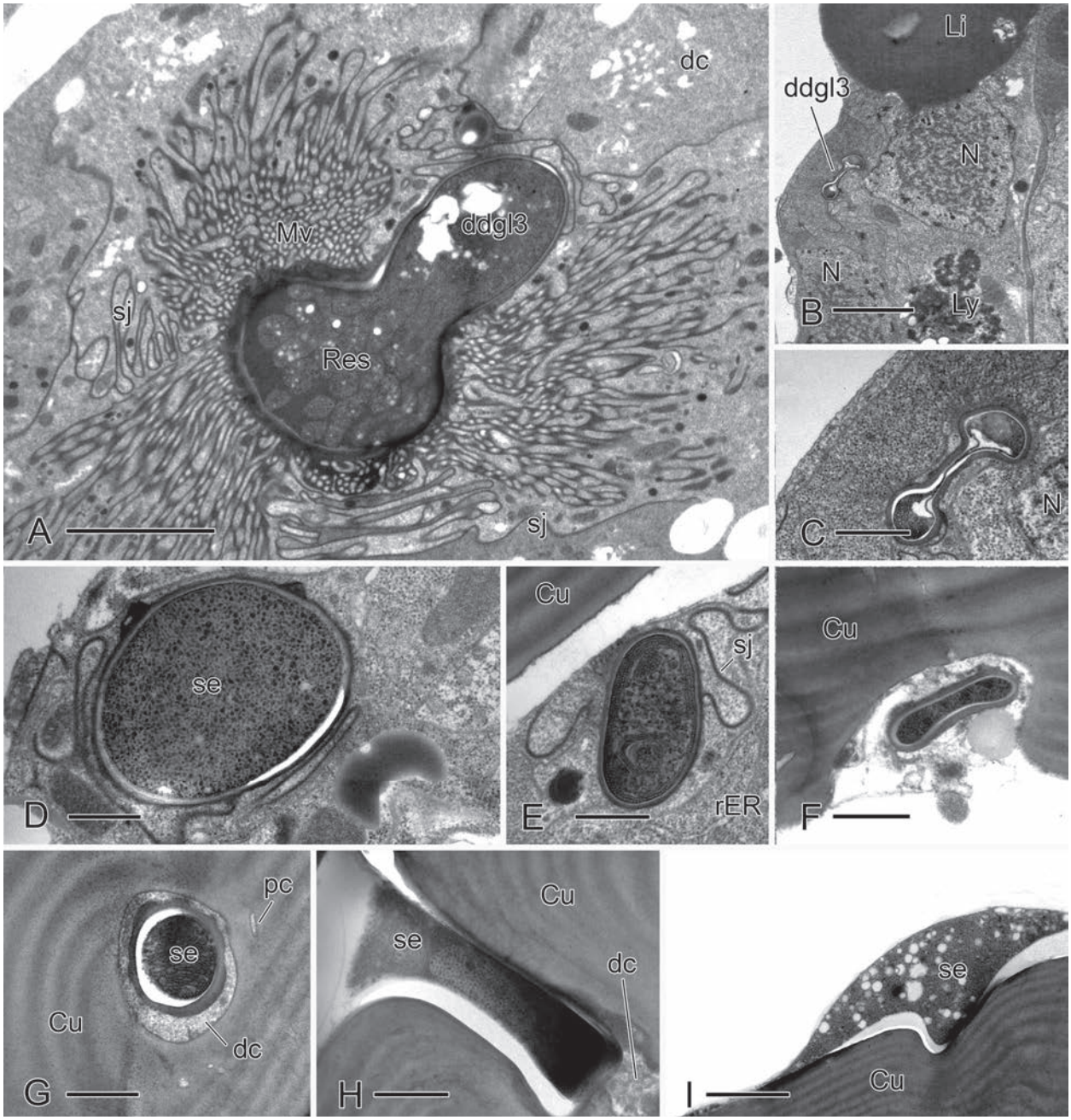

▲ **Figure 12**. The cuticle-lined duct of a dermal gland (here dermal gland 3) becomes gradually thinner distally. (**A**) The duct starting from the reservoir. Note that the cells joining the duct do not possess apical irregularities is or microvilli. Scale bar: 2 µm. (**B**) The duct is surrounded by rather large cells (see also Fig. 7) that contain large nuclei and a granular cytoplasm with few lysosomes and conspicuous lipid inclusions. The duct is collapsed in this specimen. Scale bar: 2 µm. (**C**) Close up of same detail as in the preceding figure. Note granular cytoplasm of the duct cell. Scale bar: 0.5 µm. (**D**) Here the duct is still round in cross section and is filled with secretion. Scale bar: 0.5 µm. (**E**) The duct approaches the surface cuticle. Note rough endoplasmic reticulum in the duct cell. Scale bar: 0.5 µm. (**F**) The slightly compressed duct enters the cuticle of the body surface (compare Fig. 8D). The duct cell is mostly destroyed in this specimen. Scale bar: 0.5 µm. (**G**) The duct traverses the cuticle and is first still surrounded by an extension of the duct cell. Scale bar: 0.5 µm. (**H**) A longitudinal section through the distal-most part of the duct. There is no cytoplasm anymore around the duct. Scale bar: 0.5 µm. (**I**) The secretion is deliverd from the orifice onto the surface cuticle. Scale bar: 1 µm.

Abbr.: **Cu** – cuticle (of body surface), **dc** – duct cell, **ddgl3** – duct of dermal gland 3, **Li** – lipid inclusion, **Ly** – lysosome, **Mv** – microvilli, **N** – nucleus, **pc** – pore canal, **Res** – reservoir, **se** – secretion, **sj** – septate junction.

◄ **Figure 11**. Details of dermal glands 2 (A, B, C, E, F) and 3 (D, G, H). (**A**) Gland sectioned closely beneath the reservoir. Note cell apices with irregular cell processes embedded in electron-dense material Numerous electron-lucent Golgi bodies, 'empty' vesicles and large nuclei. Scale bar: 2 µm. (**B**) Gland sectioned through the spherical reservoir (compare Fig. 10D, E). Scale bar: 2 µm. (**C**) Reservoir and surrounding apices of secretory cell. Note peculiar secretion forming 'compartments' in the reservoir. The strongly interdigitating cell membranes are provided with extensive septate junctions. Squared area is shown in Fig. 11F in higher magnification. Scale bar: 0.5 µm. (**D**) Nuclear region ...

in Fig. 13B we have tried to sum the results presented here including all the notogastral setae (except row *p*), the newly found gland orifices (the putative anterior orifice is still lacking) and our interpretations of the transversal scissures.

Further studies on these early derivative mites are evidently necessary to clarify this peculiar region of the actinotrichid mite body.

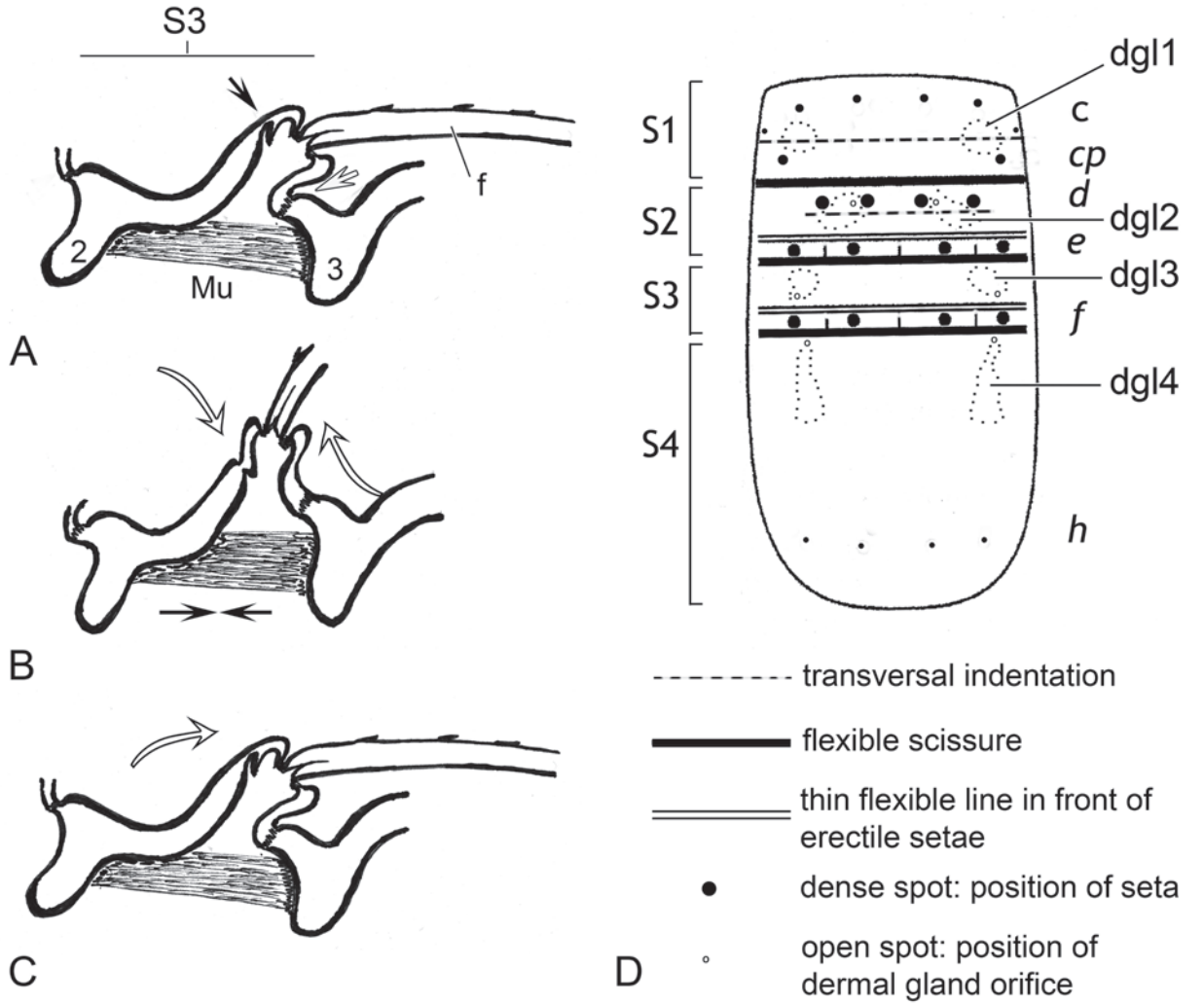

▲ **Figure 13**. Drawings depicting the suggested mechanism of seta erection (A–C) and a modified scheme of sclerites, scissures setae and dermal glands in *Heterochthonius gibbus* (D). The intercalary sclerites are considered as differentiations of the posterior borders of the sclerites 2 and 3. (**A**) Sclerite 3 in longitudinal section with a non-erected seta *f* positioned on the intercalary sclerite. Black arrow points to thin flexible line in front of the seta (= anterior border of the intercalary sclerite). Note the thin split in the procuticle. White arrow indicates flexible cuticle behind the seta (= posterior border of intercalary sclerite). (**B**) Contraction of the muscle (black arrows) induces erection (white arrows) of the seta due to the indentation of the sclerites in the region of the thin flexible line in front of the seta. (**C**) When the muscle relaxes, the seta returns to its original position (white arrow). (**D**) Scheme of a dorsal view of the notogaster (the setae *h3* and the most posterior setae *p* are not visible in this view). Note the different sizes of setae indicated by the diameter of spots, the different types of scissures with their different flexible lines and the position of yet detected orifices of dermal glands. The orifices of the most anterior pair of glands have not yet been observed. Two distinct transversal indentations are present in sclerites 1 and 2.

Abbr.: **2, 3** – apodemal ribs 2 and 3, ***c*** – setae of row *c*, ***cp*** – setae *cp*, ***d*** – setae of row *d*, dgl1-4, dermal glands 1-4, ***e*** – erectile setae of row *e* positioned on intercalary sclerites, ***f*** – erectile setae of row *f* positioned on intercalary sclerites, ***h*** – setae of row *h*, **Mu** – muscle, **S1-S4** – sclerites 1-4.

(◄ continued figure 11) of a secretory cell. Scale bar: 1 µm. (**E**) Microtubules are common in the apical cell processes. Scale bar: 0.2 µm. (**F**) Squared detail of Fig. 11C showing layered thin cuticle bordering the reservoir. Arrows point to small vesicles probably extruding dense secretion. Scale bar: 0.2 µm. (**G**) Dense material is extruded via small vesicles into the lumen traversed by apical cell processes. Scale bar: 0.5 µm. (**H**) A small nerve located in the periphery of a dermal gland cell. Scale bar: 0.5 µm.

Abbr.: **Cu** – cuticle, **Gb** – Golgi body, **Mi** – mitochondrium, **Mt** – microtubule; **Mv** – microvilli, **N** – nucleus, **ne** – nerve, **Res** – reservoir, **sj** – septate junction, **ves** – vesicle.

5. Acknowledgements

The authors wish to thank R. Ehrnsberger (University Vechta), who generously made his video-equipment available to us. The first SEM-studies were done at the Department of Cell Biology, German Cancer Research Centre, Heidelberg and we gratefully remember the kindness of N. Paweletz. Additional work was done at the EM-Center of the University Greifswald with the skilful help by R. Schlüter. We also thank the two referees for their valuable and detailed comments.

6. References

Alberti, G. & L. B. Coons (1999): Acari - Mites. – In: Harrison, F. W. (ed.): Microscopic Anatomy of Invertebrates. Vol. 8C. – Wiley-Liss, New York: 515–1265.

Alberti, G. & A. I. Moreno-Twose (2012): Fine structure of the primary eyes in *Heterochthonius gibbus* (Oribatida, Heterochthoniidae) with some general remarks on photosensitive structures in oribatid and other actinotrichid mites. – Soil Organisms **84**: 391–408.

Alberti, G. & G. Nuzzaci (1996a): SEM and TEM techniques. – In: Lindquist, E. E., J. Bruin & M. W. Sabelis (eds): Eriophyoid Mites. Their Biology, Natural Enemies and Control. World Crop Pests. Vol. 6. – Amsterdam, Elsevier Science B. V.: 399–410.

Alberti, G. & G. Nuzzaci (1996b): Internal anatomy and physiology. – In: Lindquist, E. E., J. Bruin & M. W. Sabelis (eds): Eriophyoid Mites. Their Biology, Natural Enemies and Control. World Crop Pests. Vol. 6. – Amsterdam, Elsevier Science B. V.: 101–150.

Alberti, G., V. Storch & H. Renner (1981): Über den feinstrukturellen Aufbau der Milbencuticula (Acari, Arachnida). – Zoologische Jahrbücher, Anatomie. **105**: 183–236.

Alberti, G., R. A. Norton, J. Adis, N. A. Fernandez, E. Franklin, M. Kratzmann, A. I. Moreno, G. Weigmann & S. Woas (1997): Porose integumental organs of oribatid mites (Acari, Oribatida). 2. Fine structure. – In: Alberti, G. & R. A. Norton (eds): Porose integumental organs of oribatid mites (Acari, Oribatida). – Zoologica **48/146**: 33–114.

Alberti, G., M. Heethoff, R. A. Norton, S. Schmelzle, A. Seniczak & S. Seniczak (2011): Fine structure of the gnathosoma of *Archegozetes longisetosus* Aoki (Acari: Oribatida: Trhypochthoniidae). – Journal of Morphology **272**: 1025–1079.

Coons, L. B. & G. Alberti (1999): Acari - Ticks. – In: Harrison, F. W. (ed.): Microscopic Anatomy of Invertebrates. Vol. 8B. – New York, Wiley-Liss: 267–514.

Dabert, M., W. Witalinski, A. Kazmierski, Z. Olszanowski & J. Dabert (2010): Molecular phylogeny of acariform mites (Acari, Arachnida): Strong conflict between phylogenetic signal and long-branch attraction artifacts. – Molecular Phylogenetics and Evolution **56**: 222–241.

Evans, G. E. (1992): Principles of Acarology. – C. A. B. International, Wallingford: 563pp.

Grandjean, F. (1928): Sur un oribatide pourvu d'yeux. – Bulletin de la Société Zoologique de France **53**: 235–242.

Grandjean, F. (1931): Observations sur les Oribates (2e série). – Bulletin du Muséum national d'Histoire naturelle, Paris, 2e s., **III**: 651–665.

Grandjean, F. (1934): Observations sur les Oribates (6e série). – Bulletin du Muséum national d'Histoire naturelle, Paris 2e s., **IV**: 353–359.

Grandjean, F. (1939): Les segments post-larvaires de l'hysterosoma chez les Oribates (Acariens). – Bulletin de la Société Zoologique de France **64**: 273–284.

Grandjean, F. (1947): Les Enarthronota (Acariens). Première série. – Annales des Sciences naturelles, Zoologie 11e série, **VIII**: 213–248.

Grandjean, F. (1948): Les Enarthronota (Acariens). (2e série). – Annales des Sciences Naturelles, Zoologie, 11e série, **X**: 29–58.

Grandjean, F. (1954): Essai de classification des Oribates (Acariens). – Bulletin de la Société Zoologique de France **78**: 421–446.

Hammen, L. van der (1963): The addition of segments during the postembryonic ontogenesis of the Actinotrichida (Acarida) and is importance for the recognition of the primary subdivision of the body and the original segmentation. – Acarologia **5**: 443–454.

Hammen, L. van der (1970): La segmentation primitive des Acariens. – Acarologia **12**: 3–10.

Hammen, L. van der (1980): Glossary of Acarological Terminology. Vol. I. General Terminology. – The Hague: Dr. W. Junk B. V. - Publishers: 244 pp.

Hammen, L. van der (1989): An Introduction to Comparative Arachnology. – SPB Publishing bv, The Hague: 576 pp.

Keil, Th. A. & R. A. Steinbrecht (1984): Mechanosensitive and olfactory sensilla of insects. – In: King, R. C. & H. Akai: Insect Ultrastructure 2. – Plenum Press, New York, London: 477–516.

Krantz, G. W. (2009): 3. Form and Function. – In: Krantz, G. W. & D. E. Walter: A Manual of Acarology. 3rd ed. – Texas Tech University Press, Lubbock: 5–53.

Norton, R. A. (1998): Morphological evidence for the evolutionary origin of Astigmata (Acari: Acariformes). – Experimental and Applied Acarology **22**: 559–594.

Norton, R. A. (2001): Systematic relationships of Nothrolohmanniidae, and the evolutionary plasticity of body form in Enarthronota (Acari: Oribatida). – In: Halliday, R. B., D. E. Walter, H. C. Proctor, R. A. Norton & M. J. Colloff (eds):

Acarology. Proceedings of the 10th International Congress. – CSIRO Publishing Collingwood, Australia: 58–75.

Norton, R. A. & G. Alberti (1997): Porose integumental organs of oribatid mites (Acari, Oribatida). 3. Evolutionary and ecological aspects. – In: Alberti, G. & R. A. Norton (eds): Porose integumental organs of oribatid mites (Acari, Oribatida). – Zoologica **48**/146: 115–143.

Norton, R. A., G. Alberti, G. Weigmann & S. Woas (1997): Porose integumental organs of oribatid mites (Acari, Oribatida). 1. Overview of types and distribution. – In: Alberti, G. & R. A. Norton (eds): Porose integumental organs of oribatid mites (Acari, Oribatida). – Zoologica **48**/146: 1–31.

Norton, R. A. & V. Behan-Pelletier (2009): 15. Oribatida. – In: Krantz, G. W. & D. E. Walter (eds): A Manual of Acarology. 3rd ed. – Texas Tech University Press, Lubbock: 430–564.

Norton, R. A. & M. Fuangarworn (2015): Nanohystricidae n. fam., an unusual, plesiomorphic enarthronote mite family endemic to New Zealand (Acari, Oribatida). – Zootaxa **4027**: 151–204.

Norton, R. A. & E. A. Sidorchuk (2014): *Collohmannia johnstoni* n. sp. (Acari, Oribatida) from West Virginia (U.S.A.), including description of ontogeny, setal variation, notes on biology and systematics of Collohmanniidae. – Acarologia **54**: 271–334.

OConnor, B. M. (2009): 16. Cohort Astigmatina. – In: Krantz, G. W. & D. E. Walter (eds): A Manual of Acarology. 3rd ed. – Texas Tech University Press, Lubbock: 565–657.

Raspotnig, G. (2006): Characterisation of monophyletic oribatid groups by oil gland chemistry – a novel systematic approach in Oribatida (Acari). – Abhandlungen und Berichte des Naturkundemuseums Görlitz **78**: 31–46.

Raspotnig, G., G. Krisper. & R. Schuster (2003): Functinal anatomy of oil glands in *Collohmannia gigantea* (Acari, Oribatida). – Zoomorphology **122**: 105–112.

Raspotnig, G., E. Stabentheiner, E. Föttinger, M. Schaider, G. Krisper, G. Rechberger & H. J. Leis (2009): Opisthonotal glands in the Camisiidae (Acari, Oribatida): evidence for a regressive evolutionary trend. – Journal of Zoological Systematics and Evolutionary Research **47**: 77–87.

Reynolds, E. S. (1963): The use of lead citrate at high pH as an electron–opaque stain in electron microscopy. – Journal of Cell Biology **17**: 208–212.

Richardson, K. C., L. J. Jarrett & E. H. Finke (1960): Embedding in epoxy resin for ultrathin sectioning in electron microscopy. – Stain Technology **35**: 313–323.

Thurm, U. (1984): Beiträge der Ultrastrukturforschung zur Aufklärung sensorischer Mechanismen. Verhandlungen der Deutschen Zoologischen Gesellschaft **77**: 89–103.

Weigmann, G. (2001): The body segmentation of oribatid mites from a phylogenetic perspective. – In: Halliday, R. B., D. E. Walter, H. C. Proctor, R. A. Norton & M. J. Colloff (eds): Acarology: Proceedings of the 10th International Congress. – CSIRO Publishing, Melbourne: 43–49.

Weigmann, G. (2006): Hornmilben (Oribatida). – Die Tierwelt Deutschlands. Begründet 1925 von Fr. Dahl. 76. Teil. – Goecke & Evers, Keltern: 520 pp.